

The Role of AmiB and AmiC in Daughter Cell Separation

ARRESTED AND CHAINED:

The Role of AmiB and AmiC in *Pseudomonas aeruginosa*

Daughter Cell Separation

Sarra Al-Saigh, B.Sc.

McMaster University

A Thesis Submitted to the School of Graduate Studies in Partial Fulfilment of the
Requirements of the Degree Master of Science

McMaster University: Hamilton, Ontario (2012)

MASTER OF SCIENCE: Department of Biochemistry and Biomedical Science

TITLE: Arrested and Chained: The Role of AmiB and AmiC in *Pseudomonas aeruginosa*
daughter cell separation

AUTHOR: Sarra Al-Saigh B.Sc. (McMaster University)

SUPERVISOR: Dr. Lori L. Burrows

NUMBER OF PAGES: xiv, 87

Abstract:

Peptidoglycan (PG) remodelling and cell division are two important cellular processes that are the major target of antibiotics. Due to rising resistance, the need for new antibiotics today has never been greater. Therefore it is important to fill the gaps in our understanding of these two important processes in order to discover new and promising antibiotic targets. Peptidoglycan synthesis and remodelling is a highly coordinated event that involves a wide number of enzymes and processes which are not well understood. N-acetylmuramoyl-L-alanine amidases, whose function is to cleave the amide linkage between the stem peptides and the lactyl moiety of N-acetylmuramic acid, is a major class of PG-active proteins. Their role in daughter cell separation during cell division is well established in *Escherichia coli* however little is known about it in other systems. Using enzymatic assays we characterize AmiC as a novel amidase in *Pseudomonas aeruginosa*. Through mutational analysis and microscopy we show that AmiB and AmiC are required for daughter cell separation. A deletion of both enzymes results in a cell chaining phenotype with abnormal cell morphology. Transmission electron microscopy reveals that the double mutant is arrested at the septal peptidoglycan separation step. In addition to cell chaining, the $\Delta amiB/amiC$ mutant exhibits a significant increase in susceptibility to antibiotics. We also demonstrate that the LysM motif of AmiB is not required for its role in cell separation. Furthermore, the *amiB* mutant has significantly shorter cells than the wildtype indicating an additional role for the enzyme in the cell. Lastly, through a novel bioinformatics strategy we identify PA5047 as a potential PG amidase.

Acknowledgements:

I begin by expressing my sincere thanks to my supervisor Dr. Lori L. Burrows for her continued support and advice. Her guidance throughout my Masters degree was invaluable.

I would also like to thank my committee members: Dr. Marie Elliot and Dr. Murray Junop. Their constructive feedback and encouragement were very helpful throughout our meetings.

I thank all of the Burrows lab members for their help and the many unforgettable memories.

Last but not least, I would like to thank my loving parents, supportive husband and the rest of my family for their unconditional love and support.

Table for Contents

| Title | Page |
|--|------|
| Abstract | iii |
| Acknowledgements | iv |
| List of Figures | ix |
| List of Tables | x |
| List of Abbreviations and Symbols | xi |
| Academic Achievements and Attributions | xiv |

Chapter 1: Introduction

| | |
|-------------------------------|----|
| 1.1- Overview | 1 |
| 1.2- Peptidoglycan Structure | 1 |
| 1.3- Cell Division | 5 |
| 1.3.1- Divisome Formation | 6 |
| 1.4- Peptidoglycan Synthesis | 8 |
| 1.5- Peptidoglycan Synthases | 9 |
| 1.6- Peptidoglycan Hydrolases | 10 |
| 1.6.1- Muramidases | 10 |
| 1.6.2- Endopeptidases | 11 |
| 1.6.3- Carboxypeptidases | 11 |
| 1.7- Amidases | 12 |

| | |
|---------------------------------------|----|
| 1.7.1- AmpD | 12 |
| 1.7.2- AmiD | 13 |
| 1.7.3- AmiA, AmiB and AmiC | 15 |
| 1.7.4- Recruitment | 15 |
| 1.7.5- Regulation | 16 |
| 1.8- Amidases of <i>P. aeruginosa</i> | 18 |

Chapter 2- Materials and Methods

| | |
|--|----|
| 2.1- Bacterial strains and growth media | 22 |
| 2.2- DNA procedures | 22 |
| 2.3- Electroporation | 26 |
| 2.4- Deletion mutant construction | 26 |
| 2.5- Protein expression | 28 |
| 2.6- Western blot analysis | 29 |
| 2.7- Fluorescence microscopy | 30 |
| 2.8- RBB labelled <i>M. luteus</i> cells | 31 |
| 2.9- RBB dye-release assay | 31 |
| 2.10- Zymography | 32 |
| 2.11- Growth Curves | 33 |
| 2.12- Antibiotic susceptibility assay | 33 |
| 2.13- Scanning Electron Microscopy | 34 |
| 2.14- Transmission Electron Microscopy | 35 |

Chapter 3: Results

| | |
|--|----|
| 3.1- AmiC exhibits hydrolase activity against PG | 36 |
| 3.2- AmiC-YFP localizes to distinct puncta within the cell | 39 |
| 3.3- AmiB and AmiC are essential for daughter cell separation | 41 |
| 3.3.1- The <i>amiB/amiC</i> double mutant has abnormal cell morphology | 42 |
| 3.3.2- The Δ <i>amiB/amiC</i> mutant fails to separate septal PG | 42 |
| 3.4- The LysM motif is not essential for AmiB's role in daughter cell separation | 46 |
| 3.5- The Δ <i>amiB/amiC</i> mutant is more susceptible to antibiotics | 48 |
| 3.6- Identification of PA5047 as a potential PG amidase through bioinformatics | 50 |

Chapter 4: Discussion

| | |
|---|----|
| 4.1- AmiB and AmiC are essential for daughter cell separation | 53 |
| 4.2- The Δ <i>amiB/amiC</i> mutant has abnormal cell morphology | 55 |
| 4.3- The Δ <i>amiB/amiC</i> mutant is more susceptible to antibiotics | 57 |
| 4.4- AmiB unlike AmiC might be playing another role within the cell | 59 |
| 4.5- The LysM motif of AmiB is not essential for its function in daughter cell separation | 60 |
| 4.6- Comparing the amidases of <i>P. aeruginosa</i> with those from <i>E. coli</i> | 61 |
| 4.7- Strategy for finding new PG hydrolases | 64 |

Chapter 5: Conclusions and Future Directions

5.1- Future Directions 66

5.2- Conclusions 66

5.3- Significance 68

Chapter 6: References 69

| No. | List of Figures | Page |
|------------|---|-------------|
| 1 | The structure of peptidoglycan. | 3 |
| 2 | The divisome and invagination of the cell membrane during cell division. | 7 |
| 3 | The action of N-acetylmuramoyl-L-alanine amidases on peptidoglycan. | 14 |
| 4 | TEM of the <i>E. coli</i> chained mutant lacking all three amidases. | 17 |
| 5 | Sequence alignment of AmiB from <i>E. coli</i> and <i>P. aeruginosa</i> . | 19 |
| 6 | Sequence alignment of AmiC from <i>E. coli</i> and <i>P. aeruginosa</i> . | 20 |
| 7 | AmiC exhibits PG hydrolase activity in an RBB dye release assay. | 37 |
| 8 | AmiC exhibits hydrolase activity in a zymogram. | 38 |
| 9 | Localization of AmiC-YFP. | 40 |
| 10 | AmiB or AmiC is essential for daughter cell separation. | 43 |
| 11 | The $\Delta amiB/amiC$ mutant has abnormal cell morphology. | 44 |
| 12 | The $\Delta amiB/amiC$ mutant fails to separate spetal PG. | 45 |
| 13 | The LysM motif is not essential for the function of AmiB in daughter cell separation. | 47 |
| 14 | Identification of PA5047 as a potential PG amidase. | 51 |
| 15 | Characteristics of the PA5047 deletion strain. | 52 |
| 16 | Phylogenetic tree representing all the PG amidases from <i>E. coli</i> and <i>P. aeruginosa</i> . | 62 |

| No. | List of Tables | Page |
|------------|--|-------------|
| 1 | Bacterial strains and vectors | 23 |
| 2 | Oligonucleotide sequences | 27 |
| 3 | Minimum inhibitory concentration of different antibiotics against the amidase mutants | 49 |
| 4 | Amidases of <i>P. aeruginosa</i> and <i>E. coli</i> | 63 |

List of abbreviations and symbols

| | |
|----------|--|
| Δ | Deletion |
| °C | Degree(s) centigrade |
| aa | Amino acid |
| AFM | Atomic Force Microscopy |
| amidases | <i>N</i> -acetylmuramoyl-L-alanine amidases |
| Amp | Ampicillin |
| ATP | Adenosine-5'-triphosphate |
| BSA | Bovine Serum Albumin |
| Carb | Carbenicillin |
| CI | Ciprofloxacin |
| cryo-TEM | cryo-Transmission Electron Microscopy |
| CT | Cefotaxime |
| Dap | Diaminopimelic acid |
| GlcNAc | <i>N</i> -acetylglucosamine |
| Gm | Gentamicin |
| h(s) | Hour(s) |
| IM | Inner membrane |
| IPTG | Isopropyl β -D-1-thiogalactopyranoside |
| Kan | Kanamycin |
| L | Liter(s) |

| | |
|----------|--|
| LB | Lauria-Bertani broth |
| MHA | Mueller Hinton agar |
| MHB | Mueller Hinton broth |
| MIC | Minimum Inhibitory Concentration |
| min | Minute(s) |
| ml | Milliliter(s) |
| MurNAc | <i>N</i> -acetylmuramic acid |
| nm | Nanometre(s) |
| OM | Outer membrane |
| PAO1 | O1 strain of <i>Pseudomonas aeruginosa</i> |
| PBP(s) | Penicillin binding protein(s) |
| PBS | Phosphate buffered saline |
| PCR | Polymerase chain reaction |
| PG | Peptidoglycan |
| PIA | <i>Pseudomonas</i> isolation agar |
| PP | Piperacillin |
| RBB | Remazol Brilliant Blue |
| s | Second(s) |
| SDS | Sodium Dodecyl Sulfate |
| SDS-PAGE | SDS Polyacrylamide Gel Electrophoresis |
| SEM | Scanning Electron Microscopy |
| TEM | Transmission Electron Microscopy |

| | |
|-----|-------------------|
| TZ | Ceftazidime |
| UDP | Uridindiphosphate |
| VA | Vancomycin |
| WT | Wild type |
| µg | Microgram(s) |
| µl | Microliter(s) |
| µm | Micrometer(s) |

Declaration of academic achievements:

Hanjeong Harvey performed the mating and resolving of the $\Delta amiB$ mutant and the $\Delta amiB/amiC$ double mutant.

Ryan Lamers performed the antibiotic susceptibility assay.

Chapter 1: Introduction

1.1- Overview

Peptidoglycan (PG) remodelling and cell division are two essential processes that are the main target for the majority of antibiotics. Due to the rise in antibiotic resistance, there is a great need for the discovery of new antibiotic targets. However gaps in our understanding of both of these cellular mechanisms limit our discovery of new antibiotics. Therefore, we need to study these processes further in order to complete our understanding and select novel and effective antibiotic targets.

Remodelling of the peptidoglycan exoskeleton is intimately tied to the growth and division of bacteria. Enzymes that hydrolyse PG are critical for these processes. The mechanism and regulation of many PG hydrolases have remained elusive and represent a gap in our understanding of PG remodelling. *N*-acetylmuramoyl-L-alanine amidases (amidases) are important PG hydrolases that play an integral role in cell separation during division. This study examined the role of *Pseudomonas aeruginosa* amidases in daughter cell separation. We hypothesize that both AmiB and AmiC, two PG amidases, are essential for daughter cell separation.

1.2- Peptidoglycan Structure

The cell envelope of Gram-negative bacteria is composed of the inner and outer membranes, separated by the periplasm that contains the PG layer. PG acts as the cell's

skeleton, providing mechanical stability, maintaining cell shape and protecting the cell from rupture due to high internal osmotic pressures. It is composed of repeating sugar units that are cross-linked via stem peptides (Figure 1). The strand length varies among different species, with growth conditions and method of analysis; however the mean length is between 20 and 40 disaccharide units (Vollmer and Seligman, 2010; Quintela *et al.*, 1995). PG contains alternating units of two sugars: *N*-acetylmuramic acid (MurNAc) and *N*-acetylglucosamine (GlcNAc) linked by a β -(1,4)-glycosidic bond. The glycan strands terminate in GlcNAc or 1,6-anhydroMurNAc, a MurNAc derivative with an intramolecular ether linkage between C₁ and C₆ (Figure 1). The glycan strands are cross-linked through peptides attached to the lactyl group of MurNAc (Figure 1). The composition of the peptide stem differs among species; in *Escherichia coli* as well as *P. aeruginosa*, the sequence of a newly synthesized penta-peptide is L-Ala-D-Glu-*meso*-A₂pm-D-Ala-D-Ala. *meso*-A₂pm is diaminopimelic acid (Dap), an epsilon-carboxy derivative of lysine. The D-amino acids are thought to protect against attack by most peptidases.

In Gram negatives, peptidoglycan is mainly mono-layered but not homogenous; instead, it is composed of muropeptides that differ in length of the glycan strands, peptide chains or the extent of cross-linkage (Vollmer and Bertsche, 2008). The muropeptide composition of the cell wall is dependent on the growth conditions (Glauner *et al.*, 1988). Cross-linkage is increased in stationary phase cells compared to exponentially growing cells, perhaps to strengthen the cell wall (Quintela *et al.*, 1995). The glycan strands are

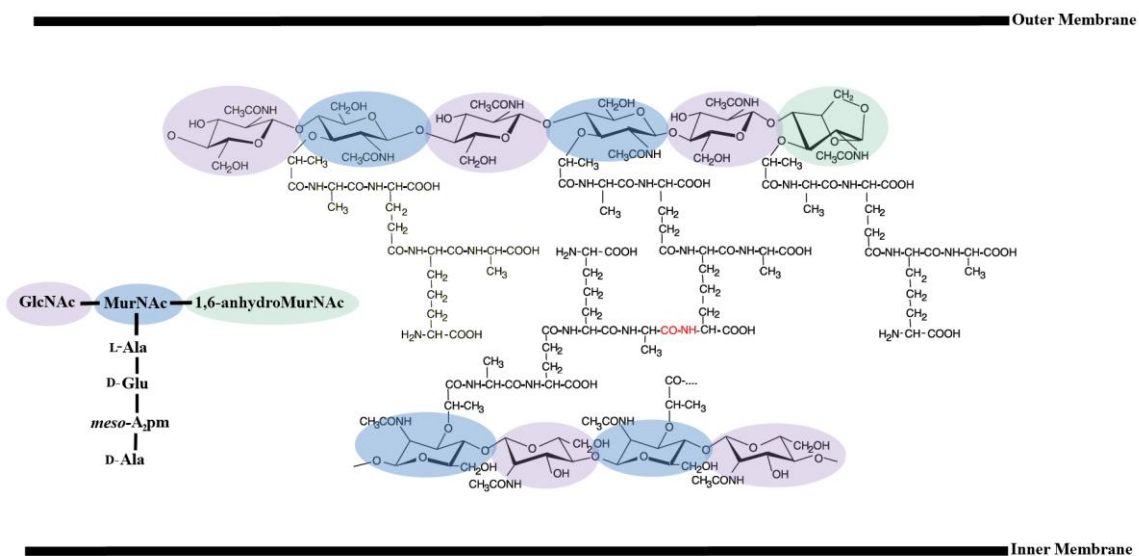


Figure 1. The structure of peptidoglycan. The cell envelope of Gram-negative bacteria is composed of the inner and outer membrane and the PG layer. PG is composed of a disaccharide monomer of *N*-acetylmuramic acid (MurNAc) and *N*-acetylglucosamine (GlcNAc) linked by a β -(1,4)-glycosidic bond. Attached to the lactyl group of MurNAc is a stem peptide. This monomer makes up one unit in a complex polymer where the stem peptides are cross-linked with one another (red) to introduce further rigidity into the structure. The chain terminates in 1,6-anhydroMurNAc, a MurNAc derivative with an intra-molecular ether linkage between C₁ and C₆ (modified from Vollmer *et al.*, 2008).

shorter in stationary phase, mean length of 17 disaccharide units (Vollmer and Seligman, 2010).

Wientjes *et al.* (1991) showed through incorporation of radiolabelled Dap in the cell wall and measuring the Dap content from a known number of cells that the average sacculus of an *E. coli* cell is composed of $\sim 3 \times 10^6$ disaccharide peptide subunits. This finding suggests that the peptidoglycan is mostly a mono-layered structure. Neutron scattering studies on isolated sacculi suggested that 75-80% of the surface of peptidoglycan is single layered and 20-25% is triple layered (Vollmer *et al.*, 2008). More advanced sample preparation techniques and application of atomic force microscopy (AFM) (Yao *et al.*, 1999) and cryo-transmission electron microscopy (cryo-TEM) (Matias *et al.*, 2003) indicated that the *E. coli* sacculus is thicker than originally thought, ~ 6 nm. Interestingly, the sacculus of *P. aeruginosa*—made of identical subunits as *E. coli*—is only 3 nm thick (Vollmer *et al.*, 2008; Matias *et al.*, 2003). This difference could be explained by the fact that sacculi include sizable regions of multilayered peptidoglycan. What is still unknown however due to limitations of the techniques available is where these regions of multi-layered peptidoglycan tend to arise and what controls their occurrence.

The PG sacculus is not rigid, but can reversibly expand and shrink up to 3-fold without rupture (Koch and Woeste, 1992). This is an important property since the PG layer encompasses the cell as it grows and provides it with resistance to internal turgor pressure. The porosity of the mesh-like sacculi was studied by Demchick and Koch

(1996). They probed intact isolated sacculi with fluorescein-labeled dextrans with a range of known molecular weights. They determined the mean effective pore radius to be 2.06 nm in *E. coli* and 2.12 nm in *Bacillus subtilis*. They also estimated that globular proteins up to ~50 kDa can diffuse through the peptidoglycan. However, these calculations were done on relaxed sacculi and it is possible that when the PG layer is expanded it might be permeable to proteins of a larger size (Vazquez-Laslop *et al.*, 2001).

Although PG is continuously being synthesized or remodelled throughout the cell's lifecycle, PG at the poles is relatively inert; PG fragments are not recycled and new fragments are not inserted (Young, 2003; de Pedro *et al.*, 1997). This inherent property of the poles is due to the way they are made during cell division.

1.3- Cell Division

Among the last steps of cell division is the formation of a septum at the division site. The septum forms from the centripetal invagination of the cytoplasmic membrane accompanied by the synthesis of new peptidoglycan, which must eventually be split for the daughter cells to separate. In Gram negative bacteria, the outer membrane is invaginated as the new peptidoglycan is laid down (Lutkenhaus, 2009). This process requires the concerted action of a variety of cell division proteins that localize at the division site into a complex called the divisome (Figure 2).

1.3.1- Divisome Formation

Divisome formation is initiated by the assembly of the Z-ring (Figure 2), a dynamic structure composed of polymers of the GTPase FtsZ, a member of the tubulin superfamily (Li *et al.*, 2013). The z-ring exerts a constrictive force on the membrane by using the energy of GTP hydrolysis. It also functions as a scaffold for divisome assembly through the sequential recruitment of numerous proteins (Goehring and Beckwith, 2005; Wissel and Weiss, 2004). The first to be recruited are FtsA and ZipA, which bind directly to the Z-ring and link it to the membrane and lead to the formation of a proto-ring (Pichoff and Lutkenhaus, 2005). Next recruited is FtsK, thought to play a role in septum closure and in excluding daughter cell chromosomes from the cell division complex (Hale and de Boer, 2002; Yu *et al.*, 1998). Subsequently, three essential proteins are recruited in a complex: FtsQ, FtsL and FtsB (Errington *et al.*, 2003). This FtsQLB complex is thought to act as a periplasmic connector between the cytoplasmic machinery and the septal PG (Rico *et al.*, 2010). Next, FtsI and FtsN are recruited. FtsI introduces peptide cross-linking into the division septum through its transpeptidase activity (Botta and Park, 1981), while FtsN promotes the stability and function of the divisome (Rico *et al.*, 2010) and is thought to trigger the constriction of the Z-ring. In addition, it has been implicated in the recruitment of the amidases to the septum (Gerding *et al.*, 2009). FtsN is a bitopic protein with a large periplasmic region containing a SPOR domain. This domain is hypothesized to interact directly with septal PG (Gerding *et al.*, 2009). Among the last proteins recruited are *N*-acetylmuramoyl-L- alanine amidases, including AmiB and AmiC

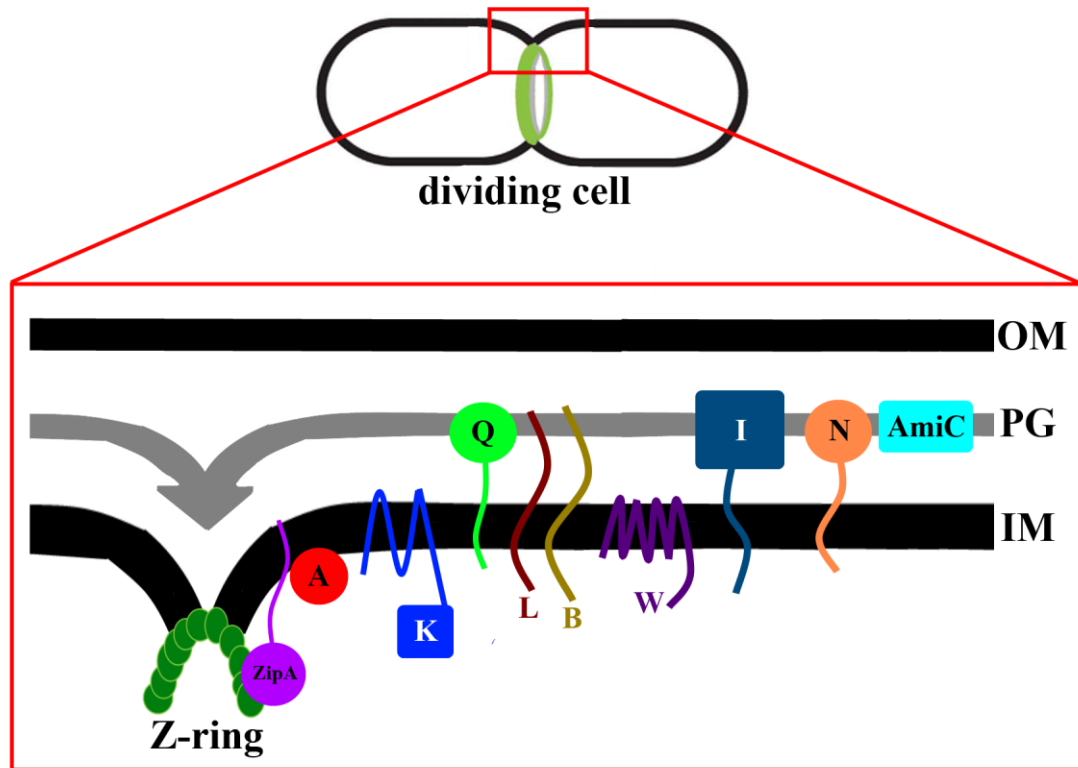


Figure 2. The divisome and invagination of the cell membrane during cell division. Schematic representation of the formation of the septum by the multimerization of FtsZ to form the Z ring. The Z ring causes the invagination of the inner membrane, the PG layer and the outer membrane sequentially. This occurs through the sequential recruitment of numerous proteins causing the formation of septal PG and cell separation. Proteins marked with letters correspond to Fts proteins.

in *E. coli*, that hydrolyze the amide bond between MurNAc and the stem peptide (Figure 2) to promote daughter cell separation (Wissel and Weiss, 2004). The recruitment of AmiC to the septum is directly dependant on FtsN (Berndhardt and Boer, 2003).

1.4- Peptidoglycan Synthesis

The synthesis of PG involves the action of a large number of cytoplasmic and membrane bound enzymes (Vollmer and Bertsche, 2008). The biosynthesis pathway is well conserved among species and can be divided into three stages: synthesis of precursor molecules in the cytoplasm, transport across the membrane and incorporation in the sacculi through a polymerization reaction.

The first stage involves the synthesis of the precursor molecules in the cytoplasm. Some of the key intermediates of precursor synthesis are the nucleotide activated amino sugars uridindiphosphate-N-acetyl-glucosamine (UDP-GlcNAc) and uridindiphosphate-N-acetyl-muramic acid (UDP-MurNAc) (El Zoeiby *et al*, 2003). The peptide side chain is formed at the lactyl group of UDP-MurNAc by the step-wise addition of L-Ala, D-Glu, m-A₂pm and a D-Ala-D-Ala dipeptide, catalyzed by ATP-dependant ligases MurC, MurD, MurE and MurF, respectively. The D-amino acids are synthesized by racemases from their respective L-amino acids (Barreteau *et al*, 2008).

Next, hydrophilic precursors are transported across the cytoplasmic membrane. MraY attaches UDP-MurNAc-pentapeptide to a C₅₅-polyisoprenoid carrier to form the

intermediate called lipid I. Subsequently, MurG adds UDP-GlcNAc to lipid I, forming the final murein precursor, lipid II (van Heijenoort, 2001). A flippase (FtsW) is responsible for transport of lipid II from the cytoplasm to the periplasmic leaflet of the cytoplasmic membrane (Mohammadi *et al.*, 2011).

1.5- Peptidoglycan Synthases

On the outer side of the cytoplasmic membrane, the lipid-linked precursors serve as substrates for the polymerization reaction, catalyzed by murein synthases which are present in 120 to 220 copies per cell (Dougherty *et al.*, 1996). All murein synthases are anchored to the cytoplasmic membrane by a single N-terminal transmembrane region. They are mainly responsible for PG polymerization and insertion into pre-existing sacculi (Sauvage *et al.*, 2008). The periplasmic portion has transpeptidase activity, or both transglycosylase and transpeptidase activities. The N-terminal transglycosylase domain catalyzes the elongation of glycan chains. The C-terminal transpeptidase domain catalyzes crosslinking between adjacent peptides. Cross-linking of the glycan strands usually takes place between the carboxyl group of D-Ala at position 4 and the amino group of the neighbouring Dap at position 3, either directly or through a short peptide bridge (Vollmer *et al.*, 2008). The DD-crosslinks are formed by DD-transpeptidases and account for the majority of the crosslinks in PG. DD-transpeptidases cleave the D-Ala at position 5 of the donor peptide and use the bond energy for crosslinking D-Ala at position

4 with *meso*-A₂pm at position 3. LD-crosslinks, which link adjacent Dap residues, are generated by an LD-transpeptidase and are less common.

1.6- Peptidoglycan Hydrolases

Bacteria have a number of PG hydrolases that are capable of cleaving covalent bonds in the PG sacculi. These enzymes are involved in a variety of physiological functions such as regulation of cell wall growth, turnover of PG during growth, separation of daughter cells during cell division, and autolysis (Vollmer *et al.*, 2008). Among those are muramidases (cleave murein), endopeptidases (cleave within the peptide bond), carboxypeptidases (hydrolyses a peptide bond at the carboxy-terminal) and amidases which cleave the amide bond linking the peptide stem to MurNAc.

1.6.1- Muramidases

The β 1,4-glycosidic linkage between MurNAc and GlcNAc can be cleaved in two ways, by lysozymes or by lytic transglycosylases. Lysozyme-type enzymes hydrolyse the glycosidic bond resulting in a product with a terminal-reducing MurNAc residue. Lytic transglycosylases cleave the glycosidic bond with a concomitant intramolecular transglycosylase reaction that generates a 1,6-anhydro ring at the MurNAc residue (Holtje *et al.*, 1975) (Figure 1). Muramidases have different substrate specificities: some cleave only PG containing peptides linked to the glycan strands, while others do not have

this requirement. Most of these enzymes either are localized to the periplasm or are attached to the inner leaflet of the outer membrane (Vollmer *et al.*, 2008).

1.6.2- Endopeptidases

Endopeptidases cleave amide bonds between amino acids in PG or its soluble fragments (Holtje, 1995). A peptidase is an enzyme that cleaves the bond between the α -carboxylic group of one amino acid and the α -amino group of another. Endopeptidases cleave within the peptide (Vollmer *et al.*, 2008). DD-peptidases cleave between two D-amino acids, whereas LD- or DL-peptidases cleave between L- and D-amino acids (Smith *et al.*, 2000). DD-endopeptidases hydrolyse the D-Ala-*meso*-A₂pm cross-bridges formed by PG synthases.

1.6.3- Carboxypeptidases

Carboxypeptidases remove the C-terminal D-Ala residues of the pentapeptide stem. Pentapeptides can act as donors and acceptors in transpeptidation reactions, while the tetrapeptide can serve only as an acceptor in DD-crosslinks. Therefore carboxypeptidases control the extent of cross-linking within the sacculi. DD-carboxypeptidases are among the most abundant of the hydrolases (Vollmer *et al.*, 2008). LD-carboxypeptidases cleave between L- and D-amino acids and are specific for the link between *meso*-A₂pm and D-Ala, degrading tetrapeptides to tripeptides. Although LD-

carboxypeptidase activity has been detected in several bacteria, few proteins have been identified. One example, encoded by the *dacB* gene, was first characterized in *Lactococcus lactis* (Courtin *et al.*, 2006). Another example is LdcA, found in *E. coli* and whose structure has been solved in *P. aeruginosa* (Korza and Bochtler, 2005).

1.7- Amidases

N-acetylmuramoyl-L-alanine amidases (amidases) cleave the amide bond between MurNAc and the N-terminal L-Ala residue of the stem peptide (Vollmer *et al.*, 2008) (Figure 3). They remove pentapeptides, tetrapeptides, tripeptides, cross-linked peptides etc. Amidases are metallopeptidases that require Zn^{2+} for their enzymatic activity and are located either in the cytoplasm or periplasm. Cytoplasmic amidases are involved in PG recycling (Lee *et al.*, 2009), while periplasmic amidases have been shown to play a role in daughter cell separation and may have additional roles. Most available studies are in *E. coli*, where 5 amidases have been identified.

1.7.1- AmpD

In *E. coli*, AmpD is a cytoplasmic protein involved in PG recycling. It cleaves the stem peptide from 1,6-anhydro-MurNac oligopeptides as part of a series of steps to recycle PG degradation products (Bacik *et al.*, 2011). In *P. aeruginosa* there are 3 reported cytoplasmic amidases: AmpD, AmpDh2 and AmpDh3 (Moya *et al.*, 2008).

However these localization predictions were not experimentally determined and AmpDh2 has a lipoprotein signal sequence that would target it to the outer membrane. Therefore further studies are required to confirm the number and localization of the amidases in *P. aeruginosa*.

1.7.2- AmiD

The other *E. coli* amidases are located in the periplasm. AmiD is the only lipoprotein and is anchored in the outer membrane. AmiD has wide substrate specificity and can cleave intact PG as well as soluble fragments containing MurNAc, regardless of the presence of an anhydro ring. The other amidases have some specificity for particular PG structures. For example, AmpD is specific for 1,6-anhydroMurNAc and AmiA has been shown to require at least a tetra-saccharide as a substrate (Lupoli *et al.*, 2009).

Although the function of AmiD is not clearly established, its crystal structure has been solved in 3 different conformations (Kerff *et al.*, 2010) to investigate its mechanism of action. The general mechanism involves nucleophilic attack of the amide bond, producing a tetrahedral conformation of the amide carbon that is stabilized by the Zn²⁺ ion. Subsequently, a proton transfer takes place, causing nitrogen to be the leaving group (Kerff *et al.*, 2010). This reaction hydrolyzes the amide bond releasing the peptide chain from the sugar backbone of PG.

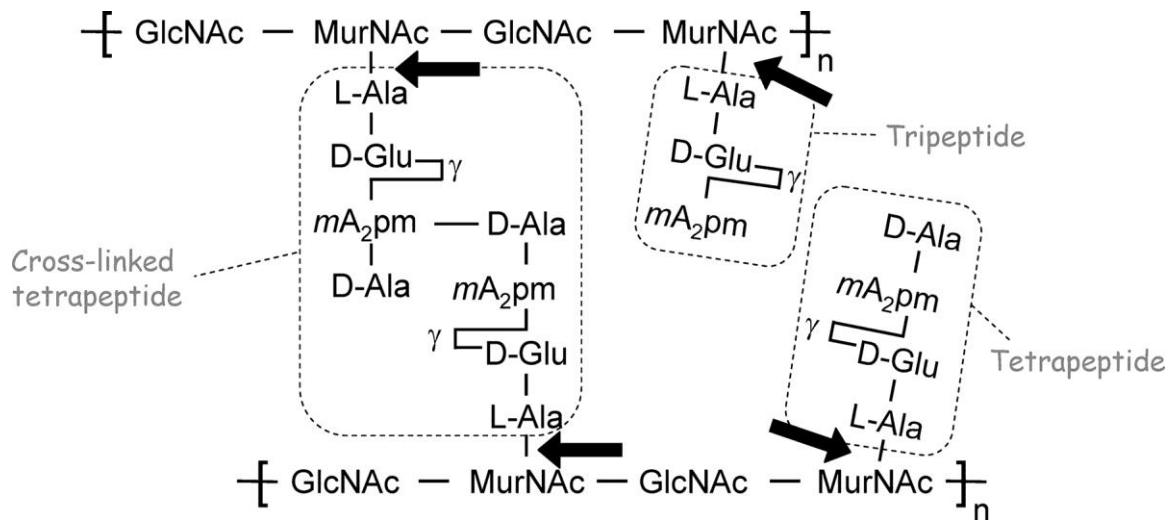


Figure 3. The action of N-acetylmuramoyl-L-alanine amidases on peptidoglycan.

Schematic depicting the structure of PG. Amidases cleave the amide linkage between the peptide stem and MurNAc. This activity can be carried out on cross-linked peptides, penta-peptides, tetra-peptides, tri-peptides etc (Pennartz *et al.*, 2009).

1.7.3- AmiA, AmiB and AmiC

AmiA, AmiB, and AmiC were characterized by Heidrich *et al.* in 2001, when they demonstrated that a triple mutant lacking these amidases grew as chains. Although some chaining is observed in double mutants, the majority of cells are able to separate. This suggests that the three amidases can compensate for one another. Electron microscopy images show that chained cells have separate inner membranes and septal PG. However there was no indication of cleavage of septal PG, therefore invagination of the outer membrane is minimal (Figure 4) (Heidrich *et al.*, 2001).

AmiA and AmiC are secreted to the periplasm via the Tat system, while AmiB has a Sec localization signal (Bernhardt and Boer, 2003). Localization studies revealed that AmiA and AmiC are diffuse throughout the periplasm, however AmiC re-localizes to the septum in dividing cells (Bernhardt and Boer, 2003). Similarly, AmiB localizes to the septum in dividing cells (Peters *et al.*, 2011). The amidases cannot be constitutively active because their unregulated activity can be detrimental to the cell. Therefore, regulatory mechanisms must target them to the right place at the right time.

1.7.4- Recruitment

In *E. coli*, the amidases are recruited to the divisome via the LytM-containing proteins, EnvC and NlpD. LytM (lysostaphin) was first identified in Gram-positive bacteria such as *Staphylococcus aureus* where it acts as an endopeptidase, relieving the

cross-linking between peptide chains (Sabala *et al.*, 2012; Ramadurai *et al.*, 1999). Although hydrolase activity has been clearly demonstrated for proteins with LytM domains, *E. coli* NlpD and EnvC lack the residues required for zinc coordination and catalysis and are inactive (Peters *et al.*, 2013). Recently, Uehara *et al.* (2010) showed that NlpD and EnvC stimulate the activities of AmiA, AmiB and AmiC. Both NlpD and EnvC localize to the septum (Peters *et al.*, 2013; Uehara *et al.*, 2009; Bernhardt and Boer, 2003), where they recruit the amidases at the last step of cell division. Therefore deletion of either of these proteins results in cell chaining, because the amidases fail to localize correctly. Recruitment is thought to proceed via FtsEX that interact with EnvC and NlpD (Yang *et al.*, 2011; Uehara and Bernhardt, 2011).

1.7.5- Regulation

Another layer of amidase activity regulation was proposed by Yang *et al.* (2012). They created a randomized mutant library of *E. coli* *amiB* and screened for constitutively active forms that caused cell lysis, releasing the plasmid encoding the mutant enzyme. Most of the recovered plasmids contained mutations that mapped to a specific helix within the active site cleft that is conserved among the amidases. This helix is thought to act as a regulatory switch. Amidases are normally found in a closed (inactive) conformation in the periplasm. Upon their recruitment to the septum, the

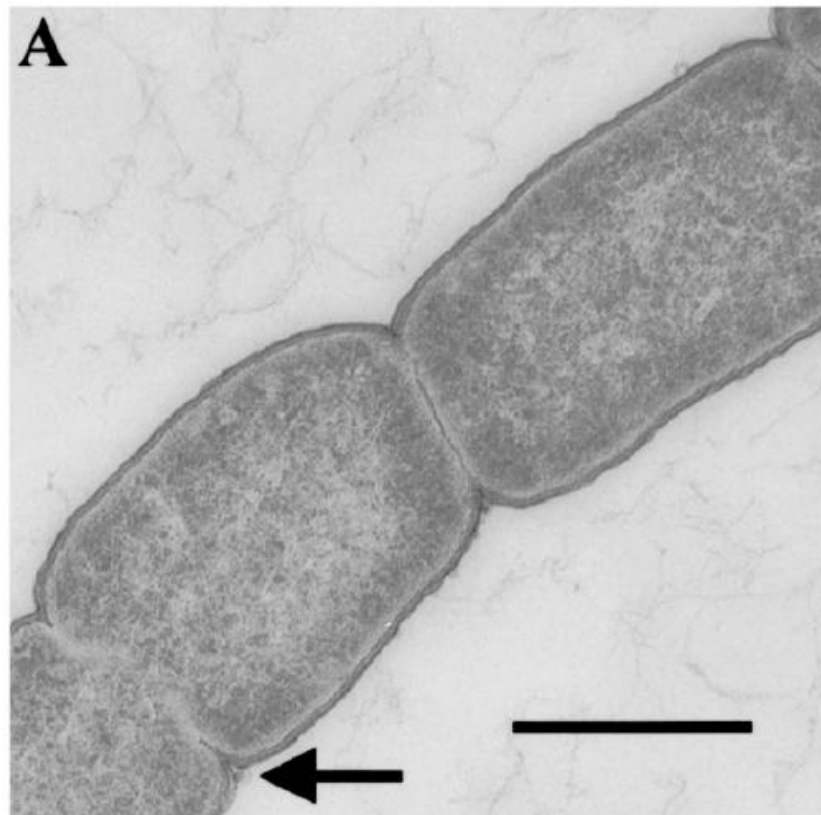


Figure 4. Transmission electron micrograph (TEM) of the *E. coli* chained mutant lacking all three amidases. An electron micrograph of murein sacculi from *E. coli* MHD52. Ultra thin section of a chain of cells. Images shows septa is formed but not cleaved. In addition, incomplete septation, where division was only initiated, can be observed (arrow). Bar represents 1 μ m. (Figure 4A from Heindrich *et al.*, 2001).

interaction of the amidase with its LytM factor is proposed to cause a conformational change that exposes the active site. It is unclear whether other organisms have similar regulatory mechanisms, and whether LytM factors are exclusively required for activation.

1.8- Amidases of *P. aeruginosa*

AmiB is the only periplasmic amidase in *P. aeruginosa* that has been characterized so far (Scheurwater *et al.*, 2007). AmiC from *P. aeruginosa* (PA5538) is a putative amidase that was identified based on its homology to *E. coli* AmiC; they share 42% identity and 59% similarity (Figure 6). AmiC is annotated as AmiA in the *Pseudomonas* genome database, but based on sequence similarity; it is more similar to *E. coli* AmiC.

A key difference between *E. coli* AmiB and its *P. aeruginosa* homologue is that the latter has a PG-binding LysM motif at its C-terminus (Scheurwater *et al.*, 2007) (Figure 5). LysM (lysine motif) is a peptidoglycan-binding domain found in many PG hydrolases (Andre *et al.*, 2008). An example of an amidase with a LysM domain is AmiB (periplasmic amidase) of *Vibrio anguillarum*. AmiB is the only periplasmic amidase that has been identified in that species, and contains three tandem LysM domains at its C-terminus that are important for its cell separation function (Ahn *et al.*, 2006). A single knockout in this gene causes cell chaining (Ahn *et al.*, 2006). It is unclear whether the LysM domains in this protein are responsible for its targeting to the septum.



Figure 5. Sequence alignment of AmiB from *E. coli* and *P. aeruginosa*. Amino acids in black and grey represent conserved sequences and similar amino acids respectively. Sequences in green represent the Sec localization signal while blue represents the LysM motif. Residues in red are conserved residues that have been shown to be essential for the activity of the enzyme (Shida *et al.*, 2001).

Even though LysM motifs are common, their sequences are poorly conserved. It is unclear whether these domains are able to specifically recognize and target the protein to septal or polar PG (Andre *et al.*, 2008; Poggio *et al.*, 2010; Steen *et al.*, 2003). Some proteins have only one LysM domain (e.g. AmiB from *P. aeruginosa*) while others have repeats of LysM. The LysM motif of *P. aeruginosa* AmiB may play a role in targeting the protein to the septum, precluding the need for LysM factors for localization. Further studies need to be conducted to clarify the mechanism of recruitment and the role of LysM.

Periplasmic amidases are not well studied in *P. aeruginosa* and there are important differences in the number and features of amidases in this pathogen compared with *E. coli*. This study aims to further investigate those enzymes in *P. aeruginosa*. We hypothesize that AmiB and AmiC of *P. aeruginosa* play an essential role in daughter cell separation.

Chapter 2- Materials and Methods:

2.1- Bacterial strains and growth media

The bacterial strains and vectors used in this study are listed in **Table 1**. The growth media used is Luria Bertani (LB) base with or without agar (Invitrogen), or where indicated, *Pseudomonas* Isolation Agar (PIA) (Difco). Antibiotics were used where indicated at the following concentrations: 100 µg/ml ampicillin (Amp) for *E. coli*, 200 µg/ml carbenicillin (Carb) for *P. aeruginosa*, 15 µg/ml gentamicin (Gm) for *E. coli*, and 30 µg/ml Gm for *P. aeruginosa*, 50 µg/ml kanamycin (Kan) for *E. coli* and 250 µg/ml Kan for *P. aeruginosa*. Cultures were grown at 37°C with shaking at 200 rpm until OD₆₀₀ of 0.6 was reached unless otherwise indicated.

2.2- DNA procedures

All vectors and constructs were purified using the QIAprep spin miniprep kit (Qiagen). Polymerase chain reaction (PCR) using the Hot Start Taq Plus DNA polymerase (Qiagen) was performed using chromosomal DNA templates prepared using the Instagene matrix (Bio-Rad) according to the manufacturer's protocol. Restriction endonuclease recognition sites were designed where applicable into PCR primers which are listed in **Table 2**. Oligonucleotides were synthesized by MOBIX (Hamilton, Ontario) and used at 1 µg/µl. Annealing temperature used for PCR was 58°C and extension times

Table 1. Bacterial stains and vectors.

| Strain or vector | Relevant characteristics | Source of reference |
|--------------------------------|---|---------------------|
| <i>E. coli</i> strains | | |
| <i>E. coli</i> TOP10 | <i>F-mcrA Δ(mrr-hsdRMS-mcrBC)φ80lacZΔM15 ΔlacX74 recA1</i> <i>araD139 Δ(araleu)7697 galU galK rpsL (StrR) endA1 nupG</i> | Invitrogen |
| <i>E. coli</i> DH5α | <i>F-φ80lacZΔM15 Δ(lacZYA-argF)U169 recA1 endA1</i> <i>hsdR17(rk-, mk+) phoA supE44 thi-1 gyrA96 relA1 λ-</i> | Invitrogen |
| <i>E. coli</i> BL21(DE3) | <i>B F- ompT hsdS(rB- mB-) dcm+Tetr gal λ(DE3) endA</i> <i>Hte [argU proL Camr] [argU ileY leuW Strep/Spectr]</i> | Stratagene |
| <i>P. aeruginosa</i> strains | | |
| PAO1 WT | wild type | J. Boyd |
| PAO1 Δ <i>amiB</i> | Deletion of the <i>amiB</i> gene from the PAO1 chromosome | This study |
| PAO1 Δ <i>amiC</i> | Deletion of the <i>amiC</i> gene from the PAO1 chromosome | This study |
| PAO1 Δ <i>amiB/amiC</i> | Deletion of both the <i>amiB</i> and <i>amiC</i> gene from the PAO1 chromosome | This study |
| PAO1 pBADGr:: <i>AmiB</i> | PAO1 wildtype overexpressing the <i>amiB</i> gene through pBADGr vector | This study |
| PAO1 pBADGr:: <i>AmiC</i> | PAO1 wildtype overexpressing the <i>amiC</i> gene through pBADGr vector | This study |

| | | |
|-------------------------|--|------------------------------|
| PAO1 pBADGr::PA5047 | PAO1 wildtype overexpressing the <i>PA5047</i> gene through pBADGr vector | This study |
| PAO1 pBADGr::AmiBΔLysM | PAO1 wildtype expressing the <i>amiB</i> gene with a deletion in LysM | This study |
| PAO1 pUCP20Gm::AmiC-YFP | PAO1 expressing AmiC-YFP through pUCP20Gm vector | This study |
| PAO1 pBADGr::AmiC-YFP | PAO1 expressing AmiC-YFP through pBADGr vector | This study |
| Vectors | | |
| pBADGr | pMLBAD backbone with <i>dhfr</i> replaced with <i>aacC1</i> | Asikyan <i>et al.</i> , 2008 |
| pBADGr::AmiB | <i>amiB</i> gene insertion into the pBADGr construct | This study |
| pBADGr::AmiC | <i>amiC</i> gene insertion into the pBADGr construct | This study |
| pBADGr::AmiBΔLysM | <i>amiB</i> gene insertion into the pBADGr construct lacking the LysM domain | This study |
| pBADGr::PA5047 | <i>PA5047</i> gene insertion into the pBADGr construct | This study |
| pBADGr::AmiC-YFP | The <i>amiC</i> gene with a C-terminal YFP inserted into pBADGr construct | This study |
| pET151 | Cleavable N-terminal His-tag expression vector | Invitrogen |
| pET151::AmiB | amino acids 27-475 of the AmiB protein cloned into pET151 | This study |
| pET151::AmiC | amino acids 22-397 of the AmiC protein cloned into pET151 | This study |
| pET101 | C-terminal His-tag expression vector | Invitrogen |
| pET101::AmiB | amino acids 27-475 of the AmiB protein cloned into pET101 | This study |
| pET101::AmiC | amino acids 22-397 of the AmiC protein cloned into pET101 | This study |

| | | |
|-----------------|---|----------------------------|
| pEX18Gm | Suicide vector with a <i>sacB</i> gene | Hoang <i>et al.</i> , 1998 |
| pEX18Gm::AmiB | 1000bps up- and down-stream of the <i>amiB</i> gene cloned into pEX18Gm | This study |
| pEX18Gm::AmiC | 1000bps up- and down-stream of the <i>amiC</i> gene cloned into pEX18Gm | This study |
| pEX18Gm::PA5047 | 1000bps up- and down-stream of the <i>PA5047</i> gene cloned into pEX18Gm | This study |

ranged from 3-5 min depending on the length of the desired PCR product. Restriction endonucleases (Fermentas) were used according to the manufacturer's protocol. Where necessary gel extraction and PCR clean-up were performed using the Qiagen gel extraction kit (Qiagen) and ligations were performed with T4 ligase (New England Biolabs). Ligation mixtures were transformed into DH5 α cells and confirmed via digestion and sequencing.

2.3- Electroporation

Confirmed plasmids of interest were electroporated into *P. aeruginosa* strains (Dower *et al.*, 1988). A toothpick of freshly grown cells was scraped from an agar plate, washed with 1 ml of nuclease free water and resuspended in 200 μ l of dH₂O. A 100 μ l aliquot of the resuspended cells and 5 μ l of plasmid DNA were combined in an electroporation cuvette. The cells were electroporated at 2.5 kV and the time constant recorded. One ml of LB was added to the cuvette and incubated at 37°C for 3 h with shaking at 200 rpm. Sixty ml of the culture was plated on a 1.5 % agar plate containing appropriate antibiotics.

2.4- Deletion mutant construction

The flanking regions of the target genes (1,000 base pairs upstream and downstream) were PCR amplified. Each PCR product was cloned into the suicide vector

Table 2. Oligonucleotide sequences.

| Name | Oligonucleotide sequence |
|------------------|---|
| pEX18GmAmiBUPF | 5'-ATTGACAAGCTTGCGGGCGGAGCTGGTTCGT-3' |
| pEX18GmAmiBUPR | 5'-TCAATGGGATCCTGAGTGAAGCACCGCGTA-3' |
| pEX18GmAmiBDwnF | 5'-TCAATGGGATCCCGTTTTTCTCATGCTCCC-3' |
| pEX18GmAmiBDwnR | 5'-TAGTTCGAATTCGGTCTTGGCCAGCGCGCC-3' |
| pEX18GmAmiCUpF | 5'-GACTGCAAGCTTCGTTCGGTTCTCGCGGTTTC-3' |
| pEX18GmAmiCUpR | 5'-TGAATCGTTCGACGGCCTTCGCTGCAGCCGC-3' |
| pEX18GmAmiCDownF | 5'-TCAAGCGTTCGACCGACGAAATACCCGATTG-3' |
| pEX18GmAmiCDownR | 5'-GATTGCGAGCTCCGGATCATGCTGCACCTC-3' |
| pBADGrAmiBF | 5'-TGACGTGGTACCATGGGTTGGGGCTTGCCT-3' |
| pBADGrAmiBR | 5'-GATGACTCTAGATCACTGGGCCGCCAGGGC-3' |
| pBADGrAmiCF | 5'-GACTAAGGTACCATGAAGCGCCGTCGTCTC-3' |
| pBADGrAmiCR | 5'-AATACGAAGCTTCTAGCCGGGAGGCTGCGC-3' |
| pBADrPA5047F | 5'-CGTTACGAATTCATGAAGACCGCCTGGCTC-3' |
| pBADGrPA5047R | 5'-GACTAAAAGCTTCTAGCGTACGACTTTAAG-3' |
| pBADGrLysMF | 5'-TACGGTGAATTCATGGGTTGGGGCTTGCCT-3' |
| pBADGrLysMR | 5'-TATCCTTCTAGATCAACGCAGCGCGGCCATGCT-3' |
| pBADGrAmiCYFPF | 5'-GACTAAGAATTCATGAAGCGCCGTCGTCTC-3' |
| pBADGrAmiCYFPR | 5'-AGGCTTAAGCTTCTACTCGTCCATGCCGAGAGT-3' |
| pET101AmiBF | 5'-CACCATGGCGCAAATCAAGAGCGTG-3' |
| pET101AmiBR | 5'-CTGGGCCGCCAGGGCGGT-3' |
| pET101AmiCF | 5'-CACCATGAGCGCCAATGTACGAATC-3' |
| pET101AmiCR | 5'-GCCGGGAGGCTGCGCGCT-3' |
| pET151AmiBR | 5'-TCACTGGGCCGCCAGGGC-3' |
| pET151AmiCR | 5'-CTAGCCGGGAGGCTGCGC-3' |
| pUCP20GmAmiCF | 5'-GACTAAAAGCTTATGAAGCGCCGTCGTCTC-3' |
| pUCP20GmAmiCR | 5'-TAGTACTCTAGAGCCGGGAGGCTGCGCGCT-3' |
| pUCP20GmYFPF | 5'-GACTTATCTAGAATGGTGAGCAAGGGCGAG-3' |
| pUCP20GmYFPR | 5'-AGGCTTGAATTCCTACTCGTCCATGCCGAGAGT-3' |

(pEX18Gm) separately and the construct was verified by digestion and sequencing (MOBIX). The deletion vector was transformed into *E. coli* SM10 cells and mating of those cells with PAO1 parent strain was performed with a 9:1, 1:1 and 1:9 ratios on LB 1.5 % agar plates. The cells were plated on PIA Gm100 plates to select PAO1 cells containing the deletion vector containing a Gm resistance cassette. Colonies were then selected and resolved using LB 5 % sucrose (no salt) agar plates to cure the suicide vector. The resulting colonies were subsequently double-patched on LB and LB Gm30 plates. Cells that only grew on LB plates and failed to grow on LB Gm30 plates were selected and colony PCR performed to verify deletion of the desired gene. Primers flanking the gene of interest as well as primers that amplify the gene itself were used. The successful mutants were stored at -80 °C with 15 % glycerol.

2.5- Protein expression

The pET151 and pET101 TOPO cloning vectors (Invitrogen) were used to clone the *amiC* and *PA5047* genes. After confirmation of the construct via sequencing (MOBIX) it was transformed into *E. coli* BL21(DE3) cells. Different culture volumes were inoculated from overnight at a ratio of 1:100 and the cells were grown to an OD₆₀₀ of 0.6-0.7. Subsequently IPTG was added to a final concentration of 1 mM and the cells were incubated for 4 h at 37°C or overnight at 16°C with shaking at 200 rpm. Cells were then harvested by centrifugation at 3,993xg for 20 min and frozen at -80 °C. The pellets were thawed and resuspended in NiA buffer (50 mM sodium phosphate buffer, pH 8.0,

300 mM NaCl) and then lysed by passage 3 times through a French press at 1,000 psi. The soluble fraction was obtained by centrifugation of the whole cell lysate at 39,191xg for 40 min. The soluble fraction was loaded and passed through a Ni column at room temp using a gravity pump. Washes with increasing concentrations of imidazole (5 mM, 15 mM, 30 mM, 50 mM, 100 mM and 300 mM) were carried out and samples separated on 15 % SDS-PAGE gels. To remove remaining high molecular weight contaminants, the salt concentration was reduced to 150 mM via overnight dialysis at 4°C and the His tags removed by digesting with tobacco etch virus protease (1 mg/ml TEV, 2 h, room temperature). Subsequently, the sample was re-passed through the Ni column. The flow-through was collected and the protein concentration measured using a Nano-drop spectrophotometer. The protein was concentrated to approximately 5 mg/ml using a spin column with a 10 kDa cut-off membrane.

2.6- Western blot analysis

Whole cell lysates were prepared by diluting overnight cultures in LB with appropriate antibiotics to an OD₆₀₀ of 0.6. The cells were harvested from a 1 ml aliquot by centrifugation for 1 min at 11,688 x g in a micro-centrifuge. The pellets were re-suspended in 100 µl of 3x SDS sample buffer (80 mM Tris (pH 6.8), 5.3% (vol/vol) 2-mercaptoethanol, 10% (vol/vol) glycerol, 0.02% (wt/vol) bromophenol blue, and 2% (wt/vol) SDS] and boiled for 10 min. The samples were subsequently separated on a 15% acrylamide gel at 150 V for 1.5 h. Samples were transferred to nitrocellulose membranes

at 250 mA for 1 h. The membranes were blocked in 5% (w/v) skimmed milk in 1x phosphate buffered saline (PBS, pH 7.0) for 1 h followed by incubation in anti-GFP antibody (1:1000 dilution) at 4°C for 18 h. The membranes were washed 3 times in 1x PBS, and incubated in anti-rabbit IgG AP secondary antibody (1:3000 dilution) (Bio-Rad) as per the manufacturer's protocol. The membranes were washed 3 times in 1x PBS then developed using alkaline phosphate developing reagent (Bio-Rad), as per the manufacturer's protocol.

2.7- Fluorescence microscopy

Five ml of LB cultures were supplemented with the necessary antibiotics or 0.5 % arabinose and grown overnight (stationary phase) or subcultured from overnights to a ratio of 1:100 and grown to an OD₆₀₀ of 0.6 (log phase). Two µl of each culture was spotted onto a 1% agar disk and mounted onto a glass slide and a glass cover slip was applied. Alternatively, strains were grown overnight on LB 1.5 % agar or LB no salt 1.5 % agar and subsequently streaked onto a 1% agar disk for microscopy. Images were captured using the 63x objective (oil immersion). Images were captured using a Leica DMI 6000B deconvolution microscope attached to a Hamamatsu Orca ER-AG camera. For fluorescence microscopy a YFP filter with an excitation of 500/24nm was used. Images were processed using ImageJ.

2.8- RBB labelled *M. luteus* cells

M. luteus was obtained from the Nodwell lab. A 15 ml overnight culture of *M. luteus* cells was subcultured into 500 ml LB, and the culture was grown overnight at 30°C with shaking at 200 rpm. The cells were subsequently autoclaved and centrifuged at 3,993xg for 20 min. The pellet was resuspended in 20 ml dH₂O and heated to 50°C with stirring. Twenty ml of 200 mg RBB (resuspended in water) was added followed by 4 g of sodium sulfate and 200 mg of sodium phosphate (in 2 ml of water). The cells were stirred at 50°C for 30 min. Stained cells were centrifuged at 3,273xg for 10 min and washed repeatedly with phosphate buffer (50 mM sodium phosphate, pH 7.0) until excess dye was removed. After numerous washes, 1.5 g of pellet remained which was resuspended in 15 ml of phosphate buffer and stored at 4 °C.

2.9- RBB dye-release assay

A dye release assay (Zhou *et al.* 1988) which uses remazol brilliant blue (RBB; Sigma) which covalently binds the sugar moieties of PG. Undigested insoluble PG remains in the pellet while PG fragments released by hydrolase activity are released into the supernatant. By measuring the absorbance of the supernatant at 595 nm, enzymatic activity can be detected (Uehara *et al.*, 2010; Scheurwater *et al.*, 2006).

Five hundred µl of RBB labelled *M. luteus* cells was incubated with purified enzymes at 37°C overnight with 200 rpm shaking. Enzymes were 1 mg/ml (lysozyme and

BSA) and 0.5 mg/ml (AmiC). All reactions were run in triplicate and repeated 3 times. After incubation, samples were centrifuged at 1,677 xg for 10 min to pellet the PG. Two hundred μ l of the supernatants of the reactions were transferred to a 96 well plate and the absorbance at 595 nm read using a plate reader (Thermo Scientific- Multiskan Go) (modified from Uehara *et al.*, 2010).

2.10- Zymography

Another assay utilized to test the hydrolase activity of AmiC was zymography. RBB labelled *M. luteus* cells were embedded in the resolving SDS-PAGE gel during preparation. After electrophoresis, proteins were renatured. If the protein possesses PG hydrolase activity, it would cleave the embedded PG. Therefore, enzymatic activity could be visualized as clear zones in a background of darkly stained PG (Scheurwater *et al.*, 2007).

SDS-PAGE gels (15 %) containing 0.02 % SDS (w/v) and 0.2 % RBB labelled PG (w/v) were prepared. Purified protein samples were prepared (1 mg/ml lysozyme and BSA and 0.5 mg/ml AmiC) and boiled for 10 min in 3-times sample buffer (62.5mM Tris pH 6.8, 2% SDS, 20% glycerol, 5% β -mercaptoethanol and 0.1% Bromophenol blue). Twenty μ l of each sample was loaded onto the gel and separated for 1.5 h at 150 V. The gel was rinsed in dH₂O and incubated in approximately 300 μ l of renaturation buffer (25 mM Tris-HCl pH 8.5 and 1 % Triton X-100) at 37 °C overnight. Subsequently the gel

was stained with 1% methylene blue in 0.01 % KOH for 3 h. The gel was washed with dH₂O until clear bands appeared against a darkly stained background.

2.11- Growth curves

Overnight cultures (5 ml) were grown in LB at 37 °C. Subsequently, 5 µl of each culture was diluted into 995 µl of fresh LB. Three hundred µl of each sample, in triplicate, was transferred into the wells of a 100 well Bioscreen plate. The wells at the edges of the plate were used as sterility controls and contained 300 µl LB only. The plate was covered and incubated at medium shaking (continuous) at 37°C for 48 h in an automated shaking incubator-spectrophotometer (Bioscreen; Growth Curves USA). Optical density readings (OD₆₀₀) were taken every 1 h. Data was graphed and statistical analyses were performed using Excel.

2.12- Antibiotic susceptibility assay

Antibiotic susceptibility assays were performed using Etest strips (bioMérieux, France). Overnight bacterial cultures were subcultured 1:50 in 5 ml Mueller-Hinton broth (MHB; Becton, Dickinson and Company, Mississauga, Ontario, Canada) and grown to logarithmic phase at 37°C, with shaking at 200 rpm. Cultures were standardized to an optical density at 600 nm (OD₆₀₀) of 0.25 in MHB, and 100 µl was spread on Mueller-Hinton agar (MHA). Etest strips were overlaid and plates were incubated for 18 h at

37°C. MICs were determined as the concentration at which the zone of inhibition intersected the Etest strip. MICs were confirmed by three independent replicates, and differences 2-fold or greater in MICs compared to the control were considered significant (Cavallari *et al.*, 2013).

2.13- Scanning Electron Microscopy

The indicated strains were grown on 1.5 % LB agar supplemented with antibiotics where appropriate. Small sections of agar containing colonies of the required strain were excised and placed in fixative solution [2 % glutaraldehyde (2 % vol/vol) in 0.1 M sodium cacodylate buffer (pH 7.4; primary fixative)] overnight. The agar was rinsed twice in buffer solution and post-fixed for 1 h in 1 % osmium tetroxide in 0.1 M sodium cacodylate buffer. After the second fixation step, the samples were dehydrated through a graded ethanol series (50, 70, 70, 95, 95, 100%, 100% and 100 %) and then dried in a critical point dryer. The agar was mounted onto scanning electron microscopy (SEM) stubs, sputter coated with gold, and viewed with a Tescan Vega II LSU scanning electron microscope (Tescan USA, PA) operating at 20kV. The images were acquired using the VEGA/TESCAN software.

Cell length measurements were performed using the ROI manager tool in ImageJ. Measurements of each strain were taken of cells (defined as having a defined cell envelope and two poles) from 6 fields of view. Measurements were only taken of cells that were in the orientation of the plane. Measurements were taken from one pole to

another pole of the same cell. Statistical analysis and graphing of the data was performed using Excel.

2.14- Transmission Electron Microscopy

The bacterial strains were grown overnight on 1.5 % LB agar plates at 37°C. The plate was scraped and the cells were resuspended in PBS containing 5 % bovine serum albumin (BSA; Sigma). Samples were frozen under high pressure using a Leica EM HPF high pressure freezer (Leica, Wien, Austria) and transferred under liquid nitrogen to cryovials containing 2% osmium tetroxide in anhydrous acetone. The vials were placed into a Leica EM AFS freeze-substitution unit (Leica, Wien, Austria) for substitution at -90°C for 72 h, followed by a gradual warm up to room temperature over a period of 52 h. The samples were removed from the freeze-substitution unit and rinsed several times in 100% acetone, then infiltrated with Epon resin through a graded series (2:1 acetone:Epon, 1:1 acetone:Epon, 1:2 acetone:Epon, 100% Epon, 100% Epon) with rotation of the samples in between solution changes. The samples were transferred to embedding moulds which were then filled with 100% Epon resin and polymerized overnight in a 60°C oven. Thin sections were cut on a Leica UCT Ultramicrotome and picked up onto Cu grids. The sections were post-stained with uranyl acetate and lead citrate and then viewed in a JEOL JEM 1200 EX TEMSCAN transmission electron microscope (JEOL, Peabody, MA, USA) operating at an accelerating voltage of 80kV. The images were acquired with an AMT 4 megapixel digital camera (Advanced Microscopy Techniques, Woburn, MA).

Chapter 3- Results

3.1- AmiC exhibits hydrolase activity against PG

AmiC is predicted to be a 397 amino acid (aa) protein, slightly smaller than its *E. coli* counterpart of 447 aa (Figure 6). The catalytic domain resides in the C-terminus while the N-terminus has a periplasmic targeting signal. PRED-TAT (Bagos *et al.*, 2010) predicts that AmiC is transported to the periplasm via the twin-arginine transport pathway, similar to the *E. coli* protein (Bernhardt and Boer, 2003). To confirm that AmiC possesses hydrolase activity against PG, two qualitative assays were carried out: an RBB dye release assay and zymography. Both assays require purified protein. Therefore different N-terminally His-tagged constructs of AmiC lacking the N-terminal Tat-localization signal were constructed and purified using a Ni²⁺ column. The construct used for the assays was an AmiC truncation from amino acids 23-398 (Figure 6).

M. luteus cells were used as a source of PG and labelled with RBB. Lysozyme (1 mg/ml) was used as a positive control and bovine serum albumin (BSA) (1 mg/ml) as the negative control. In most of the literature the reported enzyme concentration used for this assay is 4 μ M (Uehara *et al.*, 2010), however due to difficulties with purification the concentration we used was 0.014 μ M. Even at low protein concentrations, AmiC had significant PG hydrolase activity compared to the BSA negative control (Figure 7).

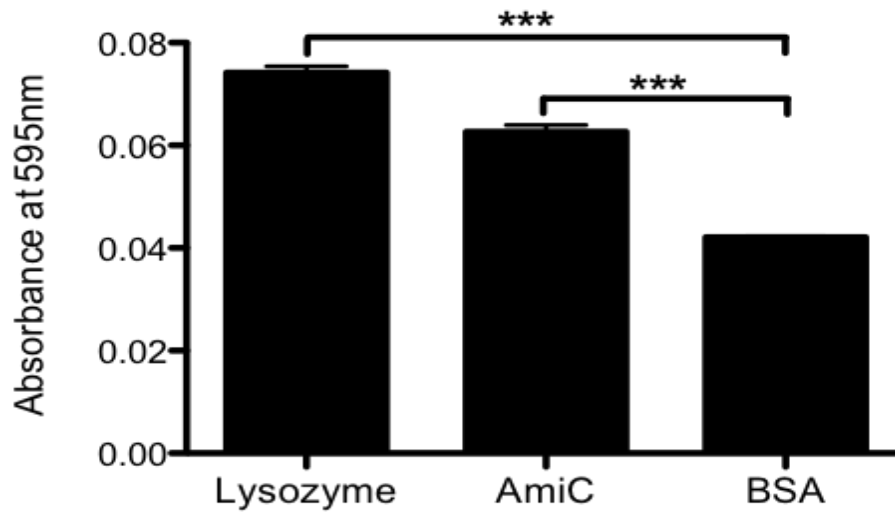


Figure 7. AmiC exhibited PG hydrolase activity in an RBB dye release assay. RBB labelled PG was incubated with different proteins in phosphate buffer. Enzymes able to hydrolase PG released dye-fragments into the supernatant which were detected by reading the absorbance at 595 nm. AmiC as well as the positive control lysozyme exhibited significant PG hydrolase activity in comparison with the negative control; BSA (n=3, P<0.001).

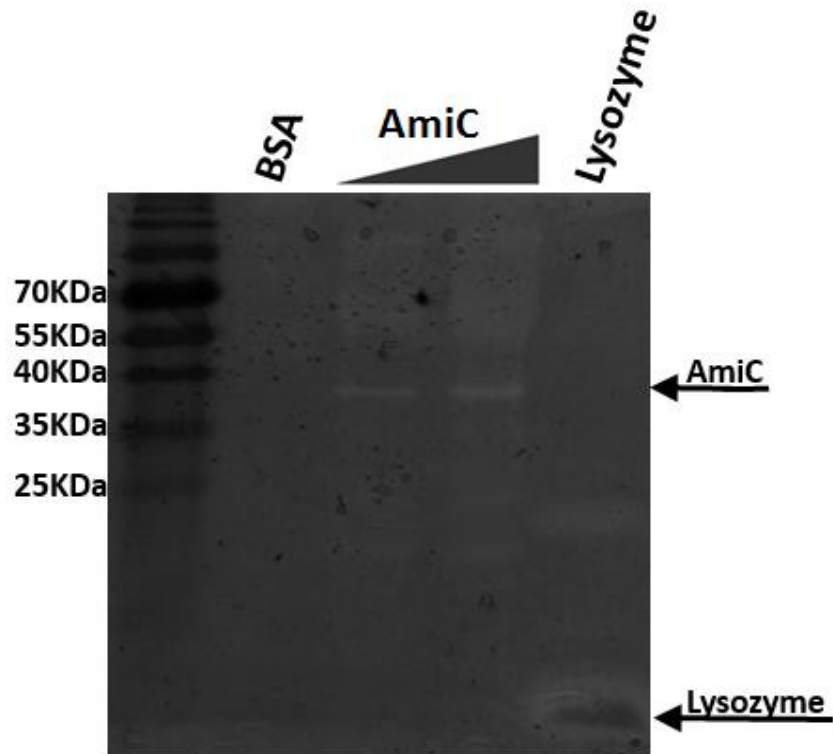


Figure 8. AmiC exhibits hydrolase activity in a zymogram. RBB-labelled *M. luteus* cells (0.02% w/v) were embedded in an SDS-PAGE gel. Lysozyme and AmiC generate zones of clearing within the darkly stained PG indicating PG hydrolase activity (n=2).

Similar to the RBB dye release assay, for zymography lysozyme was used as a positive control while BSA was used as the negative control (1 mg/ml). Preliminary results support the finding from the RBB dye release assay and suggest that AmiC has hydrolase activity against PG (Figure 8).

3.2- AmiC-YFP localizes to distinct puncta within the cell

AmiC has a Tat periplasmic localization signal. Therefore it can be tagged with a YFP tag since it will be able to fold in the cytoplasm before being transported into the periplasm (Dinh and Bernhardt, 2011). A C-terminal YFP fusion to AmiC was constructed and its integrity was verified via western blotting using an anti-GFP antibody (Figure 9A). To verify that the YFP tag did not affect AmiC function, the construct was used to complement a chained mutant. A double mutant lacking AmiB and AmiC has a chaining phenotype (below) that is restored to wild type by complementation with AmiC. The fusion was used to complement the double mutant successfully (Figure 9B).

Florescence microscopy revealed that AmiC-YFP localized to distinct puncta in both the wild type PAO1 strain and the *amiC* deletion strain (Figure 9C). This suggests that it was being targeted to specific sites within the periplasm, rather than being diffuse throughout. The YFP negative control diffused throughout the cell as expected.

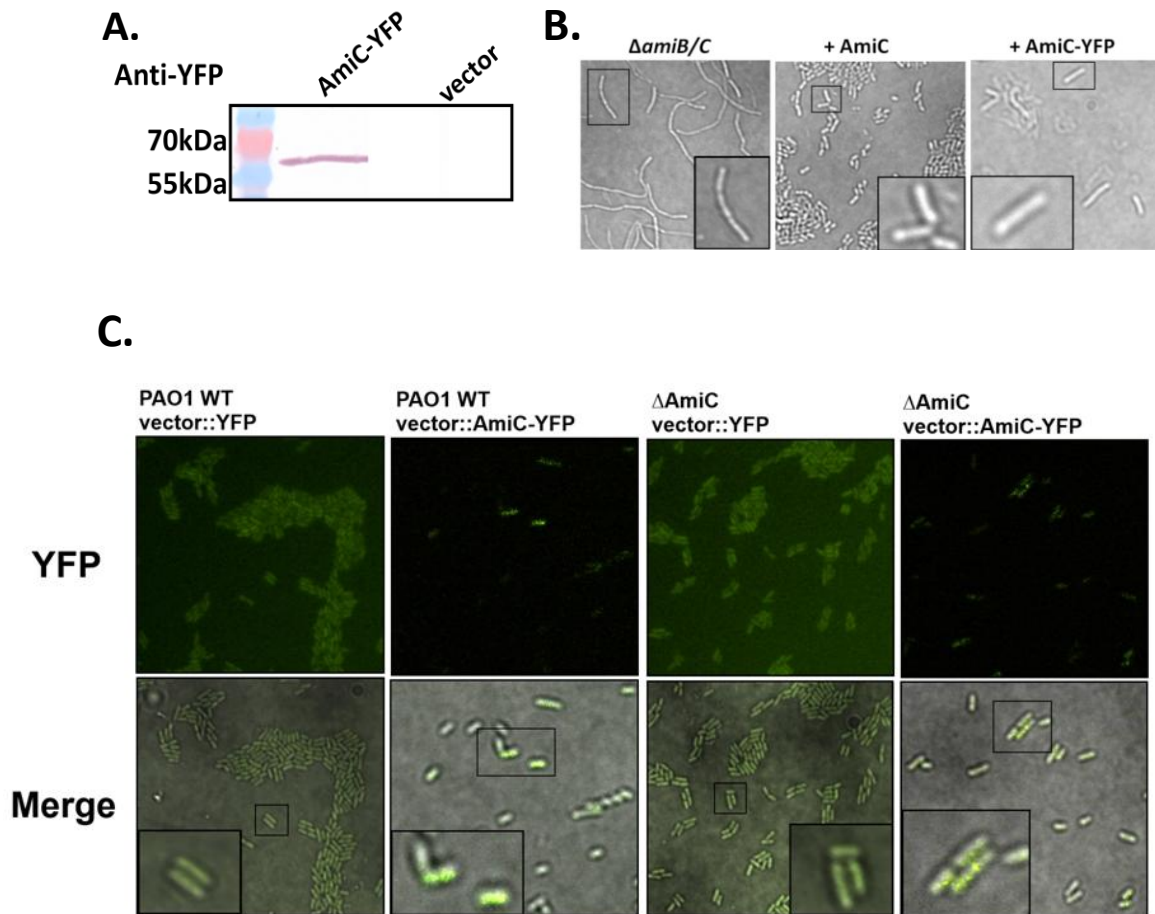


Figure 9. Localization of AmiC-YFP. (A) An anti-GFP western blot showing AmiC-YFP properly expressed at the predicted size of 68kDa. (B) Light microscopy images showing complementation of the chaining phenotype with either AmiC alone or AmiC-YFP. (C) Fluorescence microscopy pictures of different strains of *P. aeruginosa* grown in LB culture overnight and spotted onto 1% LB agar disks. Images are captured using a Leica DMI 6000B deconvolution microscope with a Hamamatsu Orca ER-AG camera under 63x magnification. Images were processed using ImageJ.

3.3- AmiB and AmiC are essential for daughter cell separation

In *E. coli*, AmiB and AmiC are important for cell division and localize to the division septum (Peters *et al.*, 2011). In addition, deletion of AmiA, AmiB and AmiC resulted in a cell chaining phenotype (Heidrich *et al.*, 2001) (Figure 4). Although the AmiB and AmiC amidases of *P. aeruginosa* are homologous to those of *E. coli*, there are some differences such as the presence of a LysM motif at the C-terminus of AmiB in *P. aeruginosa* (Figure 5). Therefore we set out to understand how cell separation occurs in *P. aeruginosa*.

The morphology of *amiB*, *amiC* and *amiB/amiC* deletion mutants was examined by light and electron microscopy. Cells were visualized in liquid culture and on agar, at log and stationary phases. Wild type PAO1 cells are mostly rod-shaped during log phase, and the *amiC* deletion mutant resembled the wild type, with no cell chaining (Figure 10A). The *amiB* mutant had rod-shaped cells and no chaining. However, the cells looked shorter and stubbier. Interestingly, the *amiB/amiC* double mutant had a profound cell chaining phenotype, with no single cells observed. Cells were in long chains, with the shortest chains observed containing 3 cells (Figure 10A). Complementation of the double mutant with either *amiB* or *amiC* abolished the cell chaining phenotype completely (Figure 10B). This result suggested that AmiB or AmiC was essential for daughter cell separation in *P. aeruginosa*, and if both enzymes were missing, cells were unable to divide.

3.3.1- The *amiB/amiC* double mutant has abnormal cell morphology

On close examination of the cell morphology of the chained double mutant, it was clear that not only was there a defect in cell separation, but the cells were of abnormal morphology. Some cells within the chain looked rod shaped, similar to the wild type, while others are very short and stumpy. The average length of *P. aeruginosa* is between 1.5 - 5µm (Holt *et al.*, 1994). The length of chained mutant cells ranged in size from ~0.16 to 2.2 µm. There were many very short, stumpy and round cells within the chain (Figure 11A). When comparing the size distribution of the cell length from the double mutant to that of the PAO1 wildtype, the double mutant had a higher percentage of abnormally short cells (Figure 11B). Around 60% of double mutant cells were 0.1 – 0.8 µm long, while more than 80% of the PAO1 wildtype cells were 0.8 – 1.6 µm. Interestingly, the $\Delta amiB$ mutant was also significantly shorter than the wild type, averaging 0.99 µm in length, while $\Delta amiC$ was similar to wildtype (Figure 11C). The reported width of *P. aeruginosa* is 0.5 – 1 µm (Holt *et al.*, 1994). There was no observable variation in width between the mutants. In addition, any variation that may have existed was too small to measure accurately with the available tools.

3.3.2- The $\Delta amiB/amiC$ mutant fails to separate septal PG

The chaining phenotype observed in an *E. coli* mutant lacking all three periplasmic amidases was attributed to the lack of cleavage of septal PG. Therefore in those mutants, the inner membranes of the future daughter cells were separated by

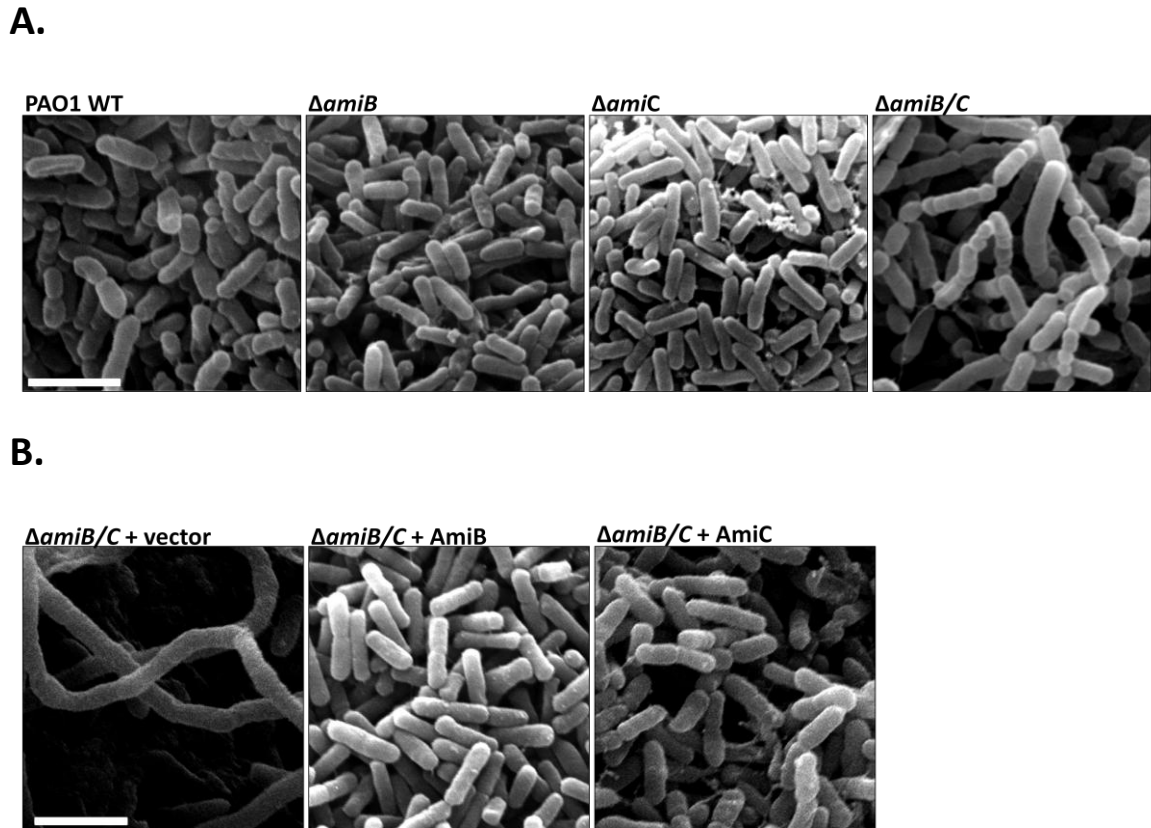
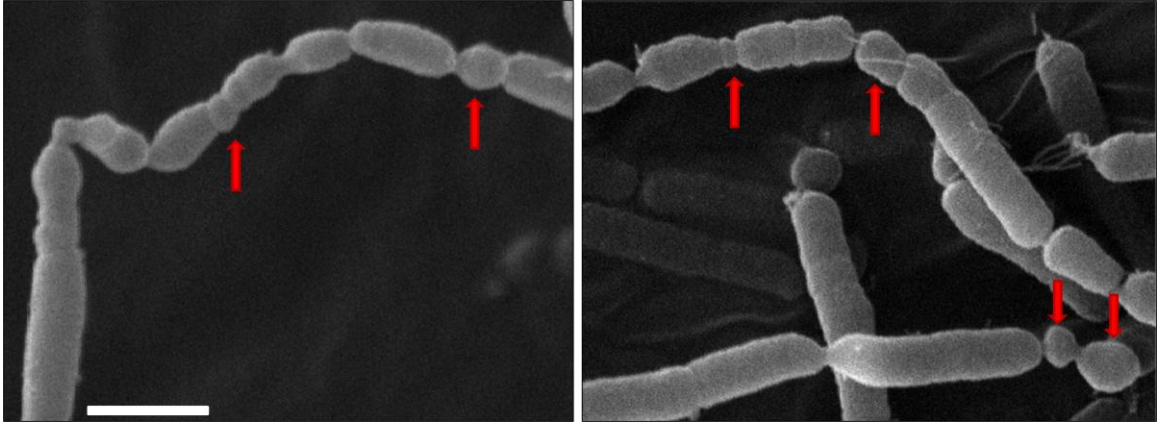
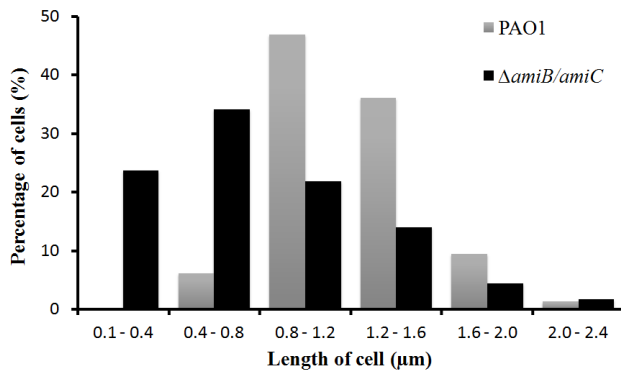


Figure 10. *AmiB* or *AmiC* is essential for daughter cell separation. Scanning electron micrograph images of the indicated strains grown on LB agar. Bar, 2 μm . **(A)** A single mutation in both *AmiB* and *AmiC* results in single cells. However a double deletion of both genes caused a cell chaining phenotype. **(B)** Complementation of the cell chaining phenotype of the double mutant by the introduction of *amiB* or *amiC*.

A.



B.



C.

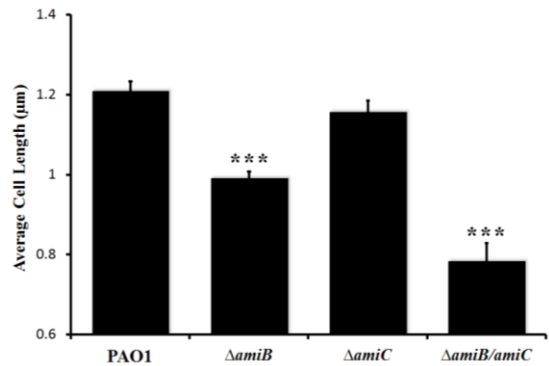


Figure 11. The $\Delta amiB/amiC$ mutant has abnormal cell morphology. (A) Scanning electron micrograph images of the chained double mutant. Red arrows point to short round cells of abnormal shape. Bar, 1 μ m. (B) Graphical representation of the difference in cell length distribution of the PAO1 WT compared to the double mutant. (C) Bar graph illustrating the average cell length of each strain. Error bars represent standard error. (***) p-value < 0.0001.

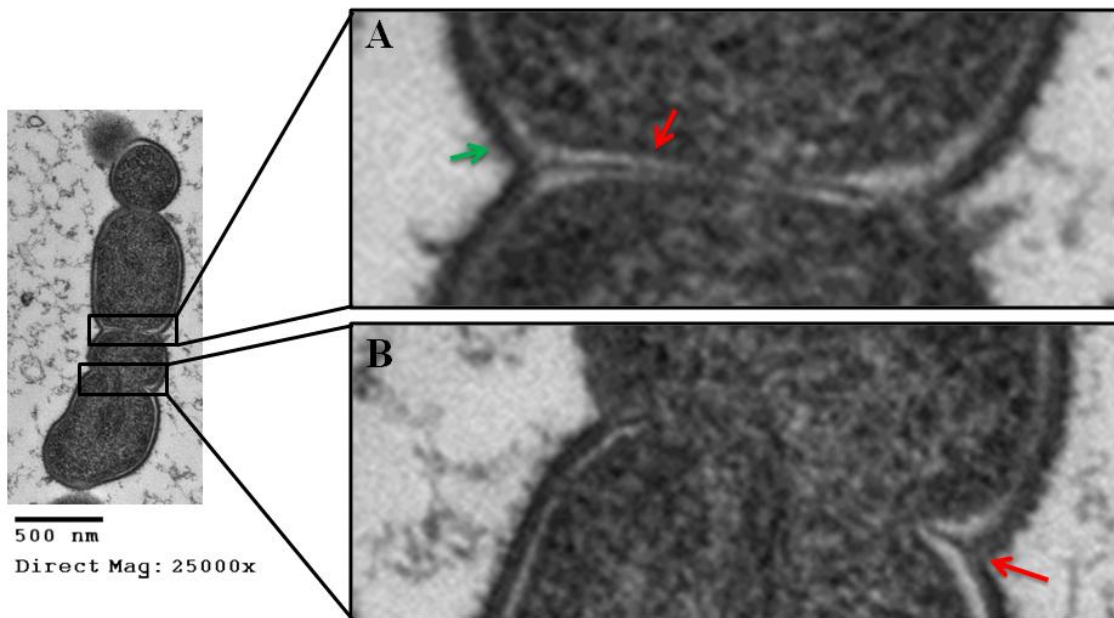


Figure 12. The $\Delta amiB/amiC$ mutant fails to separate septal PG. Transmission electron microscopy image showing a thin section of a chained mutant. (A) The septa between two unseparated daughter cells. The green arrow indicates a slightly invaginated outer membrane. The inner membrane is completely separated and the septal PG is present (red arrow). Cell division is arrested at the septal PG splitting therefore preventing the outer membrane from invagination. (B) Image of an earlier stage of division where both the inner membrane, PG layer and outer membrane are slightly invaginated (red arrow).

completely formed septal PG. However, the outer membrane was only marginally invaginated (Figure 4). To investigate whether the $\Delta amiB/amiC$ mutant was also arrested at the septal PG cleavage step, transmission electron microscopy (TEM) was performed. Cells were rapidly frozen under high pressure and subsequently sectioned into thin sections to visualize the cell wall. Interestingly TEM revealed that similar to the *E. coli* chained mutant, our double mutant was also arrested at the septal PG separation step. Electron micrograph images reveal a completely invaginated inner membrane and a completely formed septal PG. The outer membrane however was only slightly invaginated since septal PG had not separated yet (Figure 12A). There was also the presence of septa that showed both the inner and outer membranes were only slightly invaginated and no septal PG was visible (Figure 12B). These cells were likely still in the earlier stages of division and had not yet reached the septal PG separation step where they would be arrested. These findings suggested the AmiB and AmiC amidases of *P. aeruginosa* were solely responsible for septal PG separation and no other enzyme could compensate for this role if they were missing.

3.4- The LysM motif is not essential for AmiB's role in daughter cell separation

Unlike the *E. coli* protein, AmiB from *P. aeruginosa* has a LysM motif in its C-terminus (Figure 5). To investigate whether the motif was essential for the activity of AmiB, a mutant form of the *amiB* gene lacking the last 78 nucleotides encoding the predicted LysM motif was generated (*amiB*- Δ LysM). When the *amiB amiC* double

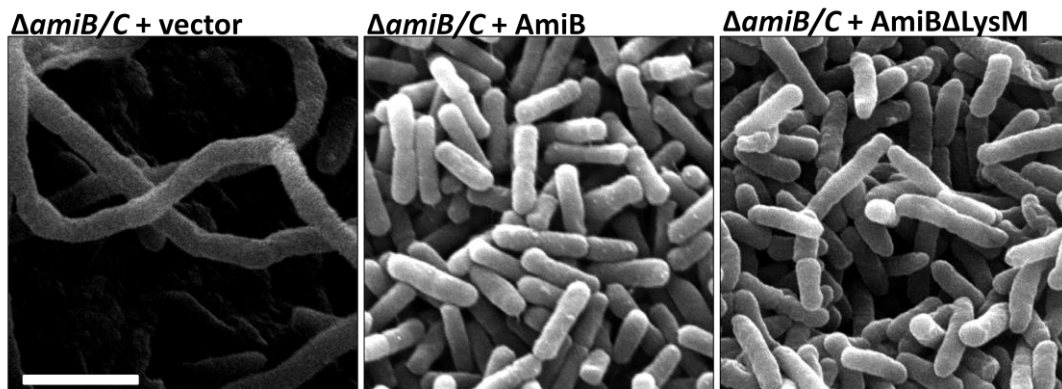


Figure 13- The LysM motif is not essential for the function of AmiB in daughter cell separation. Scanning electron microscopy images of the $\Delta amiB/amiC$ mutant complemented with either empty vector, vector carrying the full *amiB* gene or the *amiB* gene with a deletion in the C-terminal LysM motif. The deletion in the LysM motif did not inhibit the ability of AmiB from complementing the cell chaining phenotype. Bar, 2 μm .

mutant was complemented with *amiB*, the cells were able to separate. Similarly, when the double mutant was complemented with *amiB*- Δ LysM, the chaining phenotype was also eliminated (Figure 13). This suggests that the LysM motif was not essential for AmiB's function in daughter cell separation. However it may play a role in another process within the cell.

3.5- The Δ *amiB/amiC* mutant is more susceptible to antibiotics

The susceptibility of the amidase mutants to different antibiotics was tested using Etest strips. Three different types of β -lactam antibiotics were tested: piperacillin (PP), cefotaxime (CT) and ceftazidime (TZ). All of the strains had minimum inhibitory concentrations (MICs) similar to the wildtype PAO1 except for the Δ *amiB/C* double mutant. The double mutant had significantly lower MIC than the wildtype (Table 3). A fluoroquinolone antibiotic, ciprofloxacin (CI), was also tested to investigate whether this decrease in MIC was limited to β -lactams or whether it encompassed other classes of antibiotics. Interestingly, the double mutant also had a significantly lower MIC for CI (Table 3). In order to test whether this decrease in MIC was due to membrane permeability, the strain was tested with vancomycin (VA). VA is only effective against Gram-positive bacteria; due to its large structure it cannot pass through the outer membrane of Gram-negatives. Similarly to the wildtype, the double mutant and all the other strains were not susceptible to VA (Table 3). This suggests that the lower MIC exhibited by the double mutant was not due to an increase in membrane permeability.

Table 3. Minimum inhibitory concentration of the amidase mutants against different antibiotics.

| strain | Minimum Inhibitory Concentration ($\mu\text{g/ml}$) | | | | |
|-----------------------|---|----|-----|-----|------|
| | PP | CT | TZ | CI | VA |
| PAO1 | 4 | 8 | 1.5 | 1 | >256 |
| ΔamiB | 4 | 8 | 1.5 | 1 | >256 |
| ΔamiC | 4 | 8 | 1.5 | 1 | >256 |
| $\Delta\text{amiB/C}$ | 1.5 | 2 | 1 | 0.5 | >256 |

3.6- Identification of PA5047 as a potential PG amidase through bioinformatics

E. coli has four reported periplasmic amidases, while only three are predicted in *P. aeruginosa*. Therefore, we used bioinformatics to determine whether *P. aeruginosa* encoded any additional amidases that were not previously identified. The known periplasmic amidases in *E. coli* and *P. aeruginosa* were aligned to identify highly conserved sequences that might correspond to important structural motifs. Sequences that were conserved in at least four of the five enzymes were considered important. Each was used to search the *P. aeruginosa* genome, yielding several hits. Those hits were further evaluated using three criteria:

1. >20% identity overall to *P. aeruginosa* AmiB or AmiC
2. Have a potential Zn²⁺ binding site (essential for all amidases)
3. Contain a periplasmic localization signal

Twenty percent identity was selected as a cut-off because all of the known amidases share at least 30% identity. It is reported in literature that it is likely that two proteins are structurally related with less than 20% identity (Kelley and Sternberg, 2009). We selected 20% identity between sequences as a cut off as long as the candidates met other criteria.

Only PA5047 met all of these criteria. It is annotated as encoding a metallo-peptidase. Interestingly, the gene that mapped adjacent to PA5045 (*ponA*) encoding PBP1a, one of two major PG synthases in *P. aeruginosa* (Figure 14). Since genes of related function are often clustered in bacteria, this hit was particularly promising.

| | Identity to AmiB | Identity of AmiC | Zn ²⁺ binding site | Periplasmic signal | Predicted function |
|---------------|---------------------|---------------------|----------------------------------|-----------------------|-----------------------|
| PA5047 | 20.3% | 20.4% | Yes | Sec signal | Metallo- peptidase |

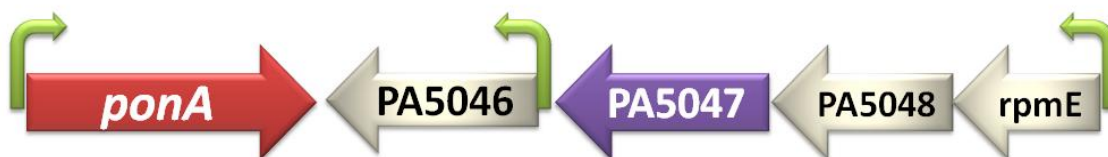


Figure 14. Identification of PA5047 as a potential PG amidase. PA5047 was the one hit that conformed to all the criteria required such as 20% identity to AmiB/AmiC and possessed a Sec localization signal as well as a Zn²⁺ binding site. Interestingly it also mapped near *ponA* which encodes PBP1a, a high molecular weight transglycosylase/transpeptidase. It is predicted to be part of the three gene operon the first of which is a ribosomal 50S protein (*rpmE*).

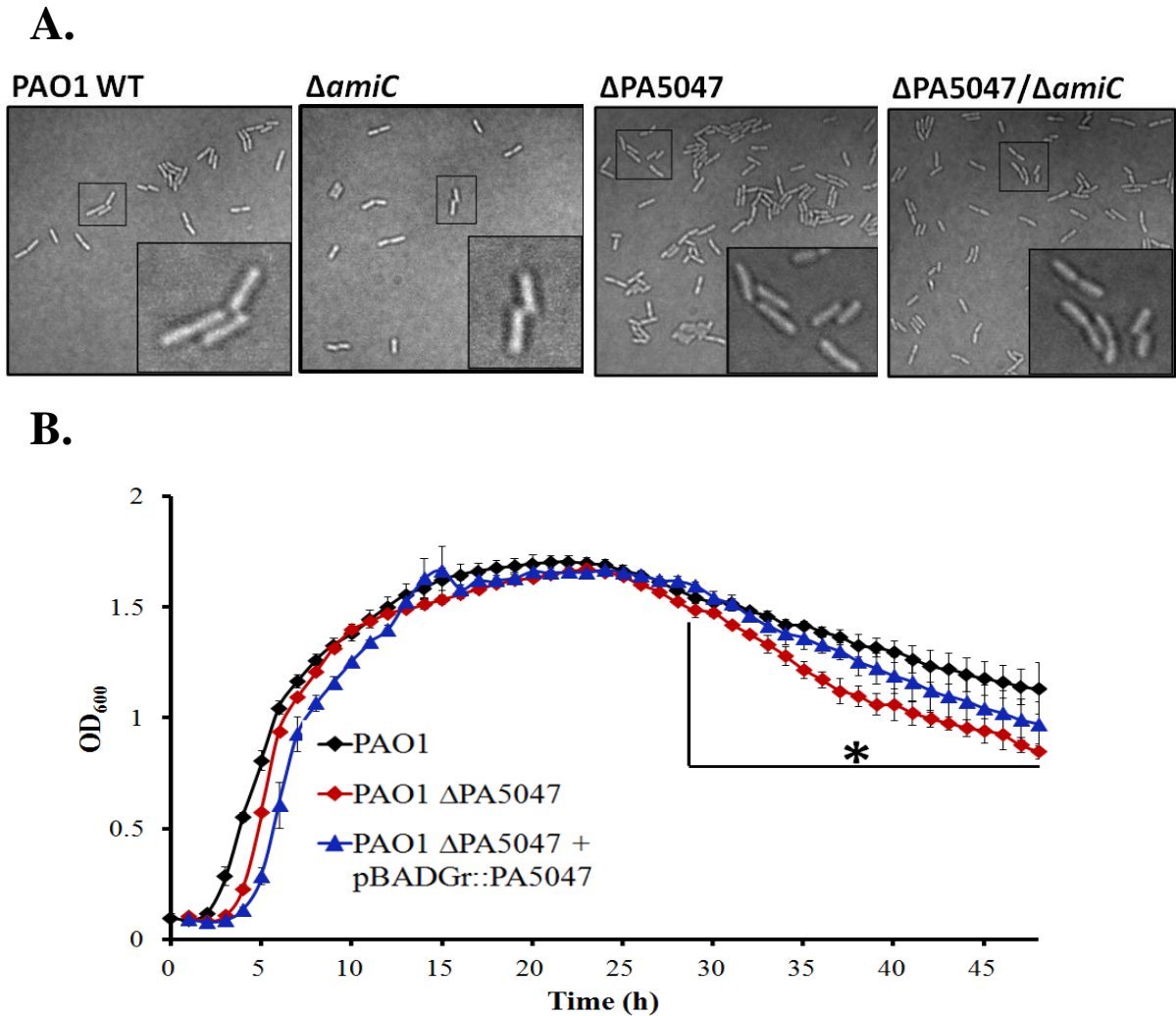


Figure 15. Characteristics of the PA5047 deletion strain. (A) Indicated strains were grown in LB culture overnight at 37°C. One microliter was spotted on a 1% LB agar disk and mounted on a microscopy slide. Cells were visualized under light microscopy. Images were processed in ImageJ. (B) A graph representing the growth curve of PAO1, the PA5047 deletion strain and the complemented deletion strain. Data was graphed using Excel. From 30 h onwards, mutant optical density was significantly less than wild type. Error bars represent standard deviation ($p < 0.05$, $n = 4$).

Interestingly, in *E. coli*, PBP1a is postulated to be involved in synthesis of lateral, not septal, PG (Mohammadi *et al.*, 2007). This may suggest that PA5047 does not play a role in cell separation, but cell elongation instead. PA5047 is predicted to be the last gene in a 3 gene operon, the first gene encoding a ribosomal 50S protein (*rpmE*).

A deletion mutant of PA5047 was constructed and combined with the *amiC* mutation. Microscopy was used to assess the cell morphology of these strains. The PA5047 deletion did not affect the shape of the cells even in combination with $\Delta amiC$ (Figure 15A). However, the PA5047 mutant typically grew more slowly than wildtype after sub-culturing from an overnight culture. This lag is reflected in the slower growth of the PA5047 mutant for the first 5 hs observed in the growth curve (Figure 15B). Interestingly and in addition to the lag in growth, the PA5047 mutant had a small but reproducible survival defect over 48 hr (Figure 15B). After 30 hr, the mutant began to deviate from the wildtype, reaching lower final density. This phenotype was rescued by complementing the mutant *in trans*.

Chapter 4- Discussion

Understanding the process of PG remodelling is of high importance since PG is a proven target for antibiotics. However, studying PG active enzymes has proven challenging because many of them have redundant functions. Prior to this study, *N*-acetylmuramoyl-L-alanine amidases were well characterized only in *E. coli*. Our study investigated the role of these enzymes in *Pseudomonas aeruginosa*. The two systems share many similarities; however, important differences are also present.

4.1- AmiB and AmiC are essential for daughter cell separation

We initially hypothesized that both AmiB and AmiC were required for daughter cell separation. However, our results indicated that AmiB and AmiC have redundant functions. The presence of either one of these amidases was sufficient for daughter cell separation to take place (Figure 10B). Deletion of both enzymes resulted in a cell chaining phenotype (Figure 10A) suggesting that no other enzyme could compensate.

Only two enzymes are involved in cell separation in *P. aeruginosa* (Figure 10). In *Vibrio anguillarum* a single amidase (AmiB) is responsible for daughter cell separation. A deletion in this *amiB* gene causes a cell chaining phenotype (Ahn *et al.*, 2006). On the other hand, three enzymes are involved in *E. coli* daughter cell separation: AmiA, AmiB and AmiC (Heindrich *et al.*, 2001). AmiA is able to compensate for the loss of AmiB and AmiC, as *amiBC* double mutants can divide. Even though there is

evidence that both AmiB and AmiC localize to the septum in dividing cells (Peters *et al.*, 2011; Bernhardt and Boer, 2003), AmiA has not been shown to localize to the septum, but is diffuse in the periplasm (Bernhardt and Boer, 2003). The localization of AmiA has not been investigated in a double mutant of AmiB and AmiC.

In *E. coli* a double mutant lacking *amiAB* divides normally (Heindrich *et al.*, 2001), suggesting that AmiC alone is sufficient to compensate for daughter separation. However a double mutant in *amiBC* or *amiAC* had a slight cell chaining phenotype (Heindrich *et al.*, 2001), suggesting that AmiC is key to normal cell division. In contrast, AmiC from *P. aeruginosa* does not seem to be the most important amidase. A single deletion in *amiC* had no effect on cell morphology while a deletion in *amiB* produced significantly shorter cells (Figure 11C).

4.2- The *amiB amiC* mutant has abnormal cell morphology

The *amiB amiC* double mutant cells were chained, indicating a defect in cell separation. In addition, they were of abnormal morphology (Figure 11A). Some of the cells were of normal cell length while others were very short and round. This abnormal morphology could also be observed in the *E. coli* triple amidase mutant (Heindrich *et al.*, 2001) however the underlying mechanism was not addressed in that study. This change in the morphology of the cells suggests that AmiB and AmiC are not simply helping to separate daughter cells, but are involved in cellular processes other than cell separation. They may be part of a complex of proteins that play a role in cell elongation. If there

were a defect in cell elongation, one would expect all the cells to become round (Iwai *et al.*, 2002). However, cell length was not uniform (Figure 11A). We propose instead that the amidase mutants have defects in localization of the site of cell division.

Localization of FtsZ is regulated by two systems: the Min system and the nucleoid occlusion system (Meinhardt and Boer, 2001). Nucleoid occlusion refers to the fact that nucleoids prevent the assembly of FtsZ in their direct vicinity. The Min system prevents division near the poles (Shih and Zheng, 2013). Since we are observing very stubby and round cells within the double mutant, it appears that division is occurring near the cell poles, similar to a defect in the Min system (Adler *et al.*, 1967). Defects in the system result in a chromosomeless mini-cell and a cell containing two copies of the chromosome.

The Min system consists of 3 proteins: MinC, MinD and MinE (Shih and Zheng, 2013). MinD and MinE interact to form a dynamic oscillator between the cell poles along with MinC. MinC is a negative regulator of FtsZ polymerization that prevents FtsZ from forming constrictions near the cell poles where MinC is most concentrated (Shih and Zheng, 2013). The biochemical reactions underlying this oscillation begin with MinD binding to ATP and then associating with the membrane as a dimer. MinC and MinE are able to bind to membrane-bound MinD, with MinE able to displace MinC from MinD. MinE stimulates the ATPase activity of MinD, whereupon both proteins detach from the membrane and migrate to the opposite pole (Loose *et al.*, 2011).

During this oscillation the MinCD complex alternately covers the cell membrane of the two cell poles. Proteins are most commonly thought to localize to their target site by the diffusion and capture mechanism (Rudner and Losick, 2010). It is thought that proteins randomly diffuse through the cytoplasm until they are recruited to a specific site within the cell. Therefore it is possible that an additional component is present at the cell poles to recruit MinD (Loose *et al.*, 2011). It has been shown that MinD does not require any other protein to bind the membrane however it binds strongly to negatively charged cardiolipin which is enriched at the cell poles (Loose *et al.*, 2011). Another proposed explanation is that MinD recognizes the negative curvature present at the cell poles directly (Huang and Ramamurthi, 2010). In the *amiB amiC* double mutant there appears to be a defect in the proper localization of the division septum. We speculate that incomplete formation of new daughter cell poles may lead to defects in MinD recruitment, and therefore in Min system function. As a result, the Z-ring may form aberrantly near the poles, giving rise to mini-cells.

4.3- The Δ *amiB/amiC* mutant is more susceptible to antibiotics

In addition to the formation of mini-cells in the chained double mutant, it also exhibits an increased sensitivity to antibiotics. The double mutant is significantly more susceptible to both the β -lactams and fluoroquinolone antibiotics tested.

β -lactams kill the cell by inactivating the penicillin binding proteins (PBPs) that function as PG synthesizing enzymes (Cavallari *et al.*, 2013). Two of the main resistance

mechanisms in *P. aeruginosa* against β -lactams are efflux pumps and β -lactamase induction (Lister *et al.*, 2009). The β -lactamase, AmpC, expression is induced in the presence of β -lactams by sensing the accumulation of PG degradation fragments (Lambert, 2002). It is possible that in the chained double mutant there is a defect in the recycling of PG fragments or their import into the cytoplasm due to the arrest of septal PG. The inability of the cell to separate the septal PG could affect the regulation of many PG active enzymes that are involved in septal PG synthesis. It is proposed that numerous PG enzymes such as PBP2, RodA, MreB, MreC and MreD are involved in pre-septal PG synthesis (Mohammadi *et al.*, 2007) and that transglycosylases play an important role in septal PG degradation during division (Uehara and Park, 2008). Therefore it is possible that during the arrest in septal PG cleavage many of these enzymes remain recruited to the septum and therefore become dysregulated, affecting the induction of AmpC. For example, in wildtype cells, AmpD is unable to process the large amount of PG degradation products because PG synthases are blocked by β -lactams, however hydrolases such as transglycosylases continue to release PG fragments (Lambert, 2002), causing the induction of AmpC. Nevertheless it is possible that some transglycosylases are arrested at the septum in the chained mutant. Therefore in the presence of β -lactams they are less active, causing the reduction in release of PG fragments thereby reducing AmpC induction and increasing susceptibility to β -lactams.

Fluoroquinolone antibiotics inhibit DNA gyrase and topoisomerase (Kohanski *et al.*, 2010). Activation of efflux pumps is the major resistance mechanism (Lee *et al.*, 2010). It is unclear why efflux would be reduced in the double mutant versus the

wildtype. Perhaps that instead of efflux the drug has more difficulty entering the cell in the double mutant. One pole of the cell has at least double layered PG. In addition, the cells are chained and there is less surface area accessible to the drug than in the single celled wildtype strain. Alternatively, due to the defect in cell division there may be a defect in chromosomal replication or segregation that affects the ability of fluoroquinolones to do their work.

4.4- AmiB might be playing another role within the cell

amiB or *amiC* single mutants formed individual cells and no chains were present (Figure 10A). However, the *amiB* mutant was significantly shorter than both the wildtype and *amiC* (Figure 11C). The wildtype and *amiC* mutant were 1.2 ± 0.2 and 1.15 ± 0.2 μm long, respectively, while the *amiB* mutant was 0.9 ± 0.2 μm . Unlike the *amiB amiC* double mutant, the decrease in length was uniform. The similar standard deviation for all three samples corresponds to the difference in length between new daughter cells and mature cells that are ready to divide (Holt, 1994). The *amiB amiC* double mutant had a standard deviation of 0.4, which corresponds to the irregularity between the cells due to the proposed mislocalization of FtsZ.

We propose that the *amiB* mutant has a defect that results in shorter cells. We propose that in addition to the role that AmiB plays in daughter cell separation, it may also play a role in daughter cell elongation. In *E. coli* the cell elongation complex is thought to be composed of PBP2, MreBCD, MraY, MurG, RodA and potentially PBP1a

(Mohammadi *et al.*, 2007). There is no evidence in the literature that a PG amidase is involved in elongation, but the reduced cell length observed for the *amiB* mutant indicates that it may be involved in ensuring that elongation is efficient or does not terminate before cells reach their optimal pre-division length.

4.5- The LysM motif of AmiB is not essential for its function in daughter cell separation

AmiB of *P. aeruginosa* has a LysM motif in its C-terminus that is not present in its *E. coli* homologue. The presence of LysM motifs in PG active enzymes is not novel and many enzymes use them for PG interactions. For example, AmiB from *V. anguillarum* has 3 tandem LysM motifs in its C-terminus (Ahn *et al.*, 2006). The exact role of these LysM motifs in *V. anguillarum* has not been investigated.

In *E. coli*, EnvC and NlpD are proteins that contain LysM domains and are responsible for recruiting the amidases to the septum (Peters *et al.*, 2011). We initially hypothesized that the LysM motif of AmiB in *P. aeruginosa* is required for its localization to the septum. However, we have shown that it is not required for the role of AmiB in cell separation (Figure 13). Therefore it is likely that AmiB is able to localize to the septum independently of its LysM domain. Recruitment might occur through EnvC, similar to the case in *E. coli* (Peters *et al.*, 2011). Open reading frame PA5133 is most similar to *E. coli envC*. In addition, PA3623 most likely encodes the NlpD homologue in *P. aeruginosa*, based on its sequence identity and its proximity to the *rpoS* gene, similar

to the genetic arrangement found in *E. coli* (Large and Hengge-Aronis, 1994). The LysM domain of AmiB may be important for another function besides cell separation.

4.6- Comparing the amidases of *P. aeruginosa* with those from *E. coli*

PG amidases are well characterized in *E. coli*. There is one cytoplasmic amidase, AmpD, and 4 periplasmic amidases: AmiA, AmiB, AmiC and AmiD. The first three are involved in daughter cell separation while AmiD has no known function in the cell and is anchored in the outer membrane.

In *P. aeruginosa*, 3 homologues of AmpD were identified: AmpD, AmpDh2 and AmpDh3 (Moya *et al.*, 2008). These amidases have been mostly studied in relation to β -lactam resistance. A mutation in AmpD causes an increased expression of AmpC, a β -lactamase (Juan *et al.*, 2006). AmpDh2 and AmpDh3 were identified as homologues of AmpD when they observed that a mutation in these genes had an additive effect when combined with an AmpD mutation (Juan *et al.*, 2006). However a critical examination of those data shows that AmpDh3 significantly increases the level of AmpC expression when combined with an AmpD mutation. However, a mutation in AmpDh2 had less effect. We propose that AmpDh2 is not a cytoplasmic amidase. Our analyses suggest that AmpDh2 is a homologue of *E. coli* AmiD (Figure 16). The Das trans-membrane prediction server predicts that the first 20 amino acids of AmpDh2 are a signal peptidase II signal sequence (Cserzo *et al.*, 1997), and that AmpDh2 is a lipoprotein. In *P. aeruginosa* the avoidance signal for the Lol outer membrane lipoprotein targeting system

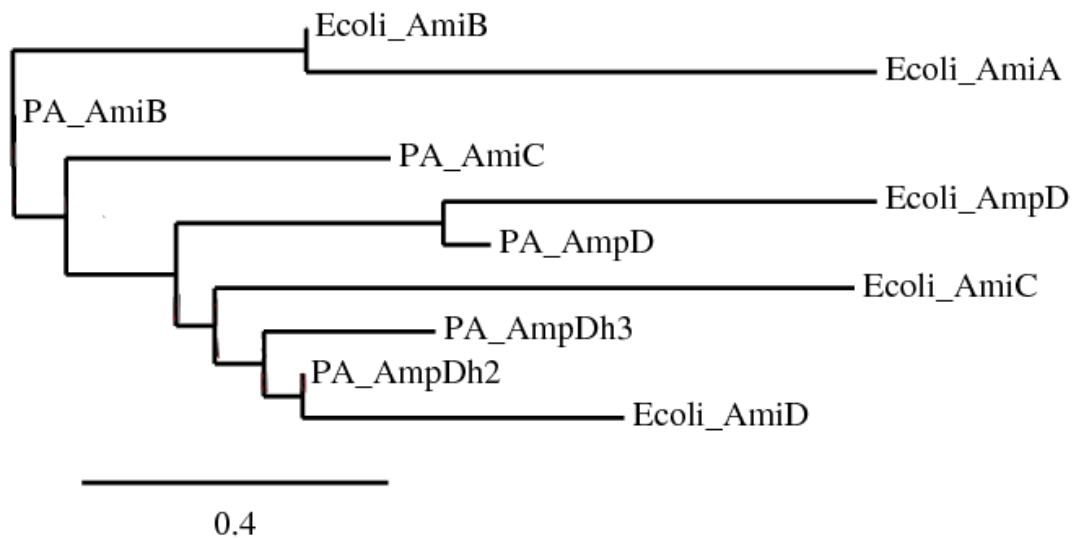


Figure 16. Phylogenetic tree of PG amidases from *E. coli* and *P. aeruginosa*.

Phylogenetic tree showing the evolutionary relationship between the sequences of PG amidases from *E. coli* and *P. aeruginosa* (PA). Branch length represents quantity of genetic change. The tree was built using Phylogeny.fr (Dereeper *et al.*, 2008).

Table 4. Amidases of *P. aeruginosa* and *E. coli*

| | <i>E. coli</i> | <i>P. aeruginosa</i> | |
|-------------|----------------|----------------------|-----------|
| | amidase | amidase | PA number |
| cytoplasmic | AmpD | AmpD | PA4522 |
| | | AmpDh3 | PA0807 |
| Periplasmic | AmiA | | |
| | AmiB | AmiB | PA4947 |
| | AmiC | AmiC | PA5538 |
| | AmiD | AmpDh2 | PA5485 |

is Lys and Ser at positions 3 and 4 (Narita and Tokuda, 2007). AmpDh2 has Ser and Phe at positions 3 and 4 respectively; therefore it is likely targeted to the outer membrane, similar to AmiD. In addition, AmiD and AmpDh2 share 53% sequence identity and map closely on a phylogenetic tree (Figure 16). We propose renaming AmpDh2 to AmiD.

Only two soluble periplasmic amidases have been identified in *P. aeruginosa*, AmiB and AmiC. AmiC (PA5538) is annotated as AmiA on the *Pseudomonas* website (www.pseudomonas.com) however Scheurwater *et al.* (2007) suggested that PA5538 is more closely related to AmiC from *E. coli* than to AmiA. In addition, AmiB and AmiA from *E. coli* are more related to one another than to AmiC (Figure 16). Table 4 shows the proposed correspondence between amidases of *P. aeruginosa* and *E. coli*.

4.7- A strategy for finding new PG hydrolases

To ensure that all potential periplasmic amidases in *P. aeruginosa* were identified, we used bioinformatics to compare highly conserved regions against the genome and then screened hits for other criteria such as predicted ability to bind Zn²⁺ and cellular localization. Using this strategy, we identified PA5047, a promising target that still needs to be validated. Our strategy may be useful to identify new PG active enzymes in other systems.

PA5047 is a periplasmic protein that is predicted to be an *N*-acetylmuramoyl-L-alanine amidase. It has a predicted Zn²⁺ ion coordination site, similar to all other PG

amidases. Interestingly, the gene is adjacent to PA5045, encoding PBP1a, a major PG synthase (Figure 14). These data suggest that PA5047 is a PG-active enzyme; however, further studies are required to confirm this prediction.

A deletion mutant of PA5047 has no phenotype, even when combined with an *amiC* mutation (Figure 15A). However, we do not know the effects a double mutation of PA5047 with *amiB* or a triple mutant also containing deletions in PA5047, *amiC* and *amiB*. As is already clear in the literature, many PG enzymes can compensate for one another. It is apparent however that PA5047 does not play a role in daughter cell separation.

Interestingly, the deletion mutant has a significant survival defect in stationary phase (Figure 15B). We hypothesized that PA5047 is perhaps expressed at stationary phase where it plays an important role. However its promoter is predicted to be a sigma70 type that also expresses a ribosomal protein (RpmE). These data suggest that PA5047 is not strictly expressed at stationary phase. The exact role of PA5047 is still unclear, and more work is required to draw firm conclusions.

Chapter 5: Conclusions and Future Directions

5.1- Future Directions

A high throughput screen can be designed to look for possible inhibitors of AmiB and AmiC. The RBB dye release assay can be optimized for high throughput and used for this purpose. In addition, to investigate whether the chained double mutant has cells with atypical chromosome distribution that is characteristic of Min mutants (Adler *et al.*, 1967), DAPI staining and microscopy can be used. We can also measure AmpC expression in the double mutant versus the wildtype using a Nitrocefin assay (van Berkel *et al.*, 2013). This is important to investigate whether AmpC levels are reduced in the double mutant as we have proposed. Lastly, the enzymatic activity of PA5047 against PG can be tested using the RBB dye release assay as well as zymography as we have done to characterize AmiC. The PA5047 mutation can also be combined with the $\Delta amiB$ mutation as well as a triple mutation with $\Delta amiC$. The cell morphology of the mutants can be assessed using microscopy.

5.2- Conclusions

Although factors involved in cell separation in *E. coli* have been characterized (Peters *et al.*, 2011; Berndhardt and Boer, 2004; Heindrich *et al.*, 2001), the process of cell separation is only beginning to be understood in other systems. Prior to this study, *P.*

aeruginosa had only one characterized PG amidase, AmiB (Scheurwater *et al.*, 2007). In this study we have characterized AmiC as another PG amidase in *P. aeruginosa*. We also showed that AmiB and AmiC are the only two amidases that play a role in daughter cell separation. In addition, the LysM motif of AmiB is not required for its role in daughter cell separation. We also proposed that the *amiB amiC* double mutant may have a defect that causes the mislocalization of the Z-ring, causing the formation of mini-cells. This hypothesis would explain the abnormal cell morphology observed in the chained mutant in *P. aeruginosa* as well as in *E. coli*. Furthermore, we demonstrated that AmiB may play another role, potentially in cell elongation, due to the significantly shorter cells observed in the *amiB* mutant. We proposed a new strategy for uncovering PG active enzymes within the genome using bioinformatics as well as specific criteria to screen our hits. Using this strategy, we discovered PA5047, predicted to be a new PG amidase.

Overall our study aims to fill the gaps in our understanding about PG remodelling and cell division in Gram-negative bacteria. We demonstrate the differences and similarities present in the *E. coli* and *P. aeruginosa* systems however understanding these processes in other organisms is vital to get a complete understanding of the system. Therefore we have proposed a strategy to facilitate finding PG amidases within bacterial genomes in order to broaden our understating.

5.3- Significance

Studying PG remodelling and cell division is very important for uncovering new antibiotic drug targets. Both of these cellular processes are the major target for antibiotics because these processes are essential for bacterial survival and are not shared with our own cells. PG remodelling is especially attractive, because the PG layer is easily accessible. Due to the rise in antibiotic resistance, the need for new antibiotic targets is greater than ever. Therefore, it is essential for us to further our understanding of both of these processes in order to discover new and promising targets.

We showed that the *amiB amiC* mutant is significantly more susceptible to antibiotics (Table 3). In addition, the chained phenotype renders *P. aeruginosa* immotile. It has been shown that motility is vital for the infectivity of *P. aeruginosa* (Campodonico *et al.*, 2009; Veesenmeyer *et al.*, 2009). Therefore a drug against both AmiB and AmiC would be great for combination therapy. It would render *P. aeruginosa* immotile and more susceptible to antibiotics, making it an easier target. The structure of AmiB from *Bartonella henselae* was solved (Yang *et al.*, 2012) and important active site residues for AmiB and AmiC are conserved (Shida *et al.*, 2001). Therefore finding a suitable drug that blocks the activity of amidases is feasible.

Chapter 6: References

- Adler, H.I., W.D. Fisher, A. Cohen, and A.A. Hardigree. 1967. Miniature *Escherichia coli* cells deficient in DNA. *Proceedings of the National Academy of Sciences of the United States of America*. 57:321-326.
- Ahn, S.K., D. ; Jeong, S. ; Hong, G. ; Kong, I. 2006. Isolation of N-acetylmuramoyl-L-alanine amidase gene (*amiB*) from *Vibrio anguillarum* and the effect of *amiB* gene deletion on stress responses. *Journal of Microbiology and Biotechnology*. 16:1416 - 1421.
- Andre, G., K. Leenhouts, P. Hols, and Y.F. Dufrene. 2008. Detection and localization of single LysM-peptidoglycan interactions. *Journal of Bacteriology*. 190:7079-7086.
- Asikyan, M.L., J.V. Kus, and L.L. Burrows. 2008. Novel proteins that modulate type IV pilus retraction dynamics in *Pseudomonas aeruginosa*. *Journal of Bacteriology*. 190:7022-7034.
- Bacik, J.P., G.E. Whitworth, K.A. Stubbs, A.K. Yadav, D.R. Martin, B.A. Bailey-Elkin, D.J. Vocadlo, and B.L. Mark. 2011. Molecular basis of 1,6-anhydro bond cleavage and phosphoryl transfer by *Pseudomonas aeruginosa* 1,6-anhydro-N-

acetylmuramic acid kinase. *The Journal of Biological Chemistry*. 286:12283-12291.

Bagos, P.G., E.P. Nikolaou, T.D. Liakopoulos, and K.D. Tsirigos. 2010. Combined prediction of Tat and Sec signal peptides with hidden Markov models. *Bioinformatics*. 26:2811-2817.

Barreteau, H., A. Kovac, A. Boniface, M. Sova, S. Gobec, and D. Blanot. 2008. Cytoplasmic steps of peptidoglycan biosynthesis. *FEMS Microbiology Reviews*. 32:168-207.

Begg, K.J., A. Takasuga, D.H. Edwards, S.J. Dewar, B.G. Spratt, H. Adachi, T. Ohta, H. Matsuzawa, and W.D. Donachie. 1990. The balance between different peptidoglycan precursors determines whether *Escherichia coli* cells will elongate or divide. *Journal of Bacteriology*. 172:6697-6703.

Bernhardt, T.G., and P.A. de Boer. 2003. The *Escherichia coli* amidase AmiC is a periplasmic septal ring component exported via the twin-arginine transport pathway. *Molecular Microbiology*. 48:1171-1182.

- Bernhardt, T.G., and P.A. de Boer. 2004. Screening for synthetic lethal mutants in *Escherichia coli* and identification of EnvC (YibP) as a periplasmic septal ring factor with murein hydrolase activity. *Molecular Microbiology*. 52:1255-1269.
- Blencowe, D.K., S. Al Jubori, and A.P. Morby. 2011. Identification of a novel function for the FtsL cell division protein from *Escherichia coli* K12. *Biochemical and Biophysical Research Communications*. 411:44-49.
- Botta, G.A., and J.T. Park. 1981. Evidence for involvement of penicillin-binding protein 3 in murein synthesis during septation but not during cell elongation. *Journal of Bacteriology*. 145:333-340.
- Campononico, V.L., N.J. Llosa, M. Grout, G. Doring, T. Maira-Litran, and G.B. Pier. 2010. Evaluation of flagella and flagellin of *Pseudomonas aeruginosa* as vaccines. *Infection and Immunity*. 78:746-755.
- Carrasco-Lopez, C., A. Rojas-Altuve, W. Zhang, D. Heseck, M. Lee, S. Barbe, I. Andre, P. Ferrer, N. Silva-Martin, G.R. Castro, M. Martinez-Ripoll, S. Mobashery, and J.A. Hermoso. 2011. Crystal structures of bacterial peptidoglycan amidase AmpD and an unprecedented activation mechanism. *The Journal of Biological Chemistry*. 286:31714-31722.

- Cavallari, J.F., R.P. Lamers, E.M. Scheurwater, A.L. Matos, and L.L. Burrows. 2013. Changes to its peptidoglycan-remodeling enzyme repertoire modulate beta-lactam resistance in *Pseudomonas aeruginosa*. *Antimicrobial Agents and Chemotherapy*. 57:3078-3084.
- Choi, K.H., and H.P. Schweizer. 2005. An improved method for rapid generation of unmarked *Pseudomonas aeruginosa* deletion mutants. *BMC Microbiology*. 5:30.
- Courtin, P., G. Miranda, A. Guillot, F. Wessner, C. Mezange, E. Domakova, S. Kulakauskas, and M.P. Chapot-Chartier. 2006. Peptidoglycan structure analysis of *Lactococcus lactis* reveals the presence of an L,D-carboxypeptidase involved in peptidoglycan maturation. *Journal of Bacteriology*. 188:5293-5298.
- Cserzo, M., E. Wallin, I. Simon, G. von Heijne, and A. Elofsson. 1997. Prediction of transmembrane alpha-helices in prokaryotic membrane proteins: the dense alignment surface method. *Protein Engineering*. 10:673-676.
- de Pedro, M.A., J.C. Quintela, J.V. Holtje, and H. Schwarz. 1997. Murein segregation in *Escherichia coli*. *Journal of Bacteriology*. 179:2823-2834.
- Demchick, P., and A.L. Koch. 1996. The permeability of the wall fabric of *Escherichia coli* and *Bacillus subtilis*. *Journal of Bacteriology*. 178:768-773.

- Dereeper, A., V. Guignon, G. Blanc, S. Audic, S. Buffet, F. Chevenet, J.F. Dufayard, S. Guindon, V. Lefort, M. Lescot, J.M. Claverie, and O. Gascuel. 2008. Phylogeny.fr: robust phylogenetic analysis for the non-specialist. *Nucleic Acids Research*. 36:W465-469.
- Diez, A.A., A. Farewell, U. Nannmark, and T. Nystrom. 1997. A mutation in the ftsK gene of *Escherichia coli* affects cell-cell separation, stationary-phase survival, stress adaptation, and expression of the gene encoding the stress protein UspA. *Journal of Bacteriology*. 179:5878-5883.
- Dinh, T., and T.G. Bernhardt. 2011. Using superfolder green fluorescent protein for periplasmic protein localization studies. *Journal of Bacteriology*. 193:4984-4987.
- Dougherty, T.J., K. Kennedy, R.E. Kessler, and M.J. Pucci. 1996. Direct quantitation of the number of individual penicillin-binding proteins per cell in *Escherichia coli*. *Journal of Bacteriology*. 178:6110-6115.
- El Zoeiby, A., F. Sanschagrin, and R.C. Levesque. 2003. Structure and function of the Mur enzymes: development of novel inhibitors. *Molecular Microbiology*. 47:1-12.

- Errington, J., R.A. Daniel, and D.J. Scheffers. 2003. Cytokinesis in bacteria. *Microbiology and Molecular Biology Reviews*. 67:52-65.
- Firczuk, M., and M. Bochtler. 2007. Folds and activities of peptidoglycan amidases. *FEMS Microbiology Reviews*. 31:676-691.
- Garcia, D.L., and J.P. Dillard. 2006. AmiC functions as an N-acetylmuramyl-l-alanine amidase necessary for cell separation and can promote autolysis in *Neisseria gonorrhoeae*. *Journal of Bacteriology*. 188:7211-7221.
- Gerding, M.A., B. Liu, F.O. Bendezu, C.A. Hale, T.G. Bernhardt, and P.A. de Boer. 2009. Self-enhanced accumulation of FtsN at Division Sites and Roles for Other Proteins with a SPOR domain (DamX, DedD, and RlpA) in *Escherichia coli* cell constriction. *Journal of Bacteriology*. 191:7383-7401.
- Glauner, B., J.V. Holtje, and U. Schwarz. 1988. The composition of the murein of *Escherichia coli*. *The Journal of Biological Chemistry*. 263:10088-10095.
- Goehring, N.W., and J. Beckwith. 2005. Diverse paths to midcell: assembly of the bacterial cell division machinery. *Current Biology*. 15:R514-526.

- Hale, C.A., and P.A. de Boer. 2002. ZipA is required for recruitment of FtsK, FtsQ, FtsL, and FtsN to the septal ring in *Escherichia coli*. *Journal of Bacteriology*. 184:2552-2556.
- Heidrich, C., M.F. Templin, A. Ursinus, M. Merdanovic, J. Berger, H. Schwarz, M.A. de Pedro, and J.V. Holtje. 2001. Involvement of N-acetylmuramyl-L-alanine amidases in cell separation and antibiotic-induced autolysis of *Escherichia coli*. *Molecular Microbiology*. 41:167-178.
- Hoang, T.T., R.R. Karkhoff-Schweizer, A.J. Kutchma, and H.P. Schweizer. 1998. A broad-host-range Flp-FRT recombination system for site-specific excision of chromosomally-located DNA sequences: application for isolation of unmarked *Pseudomonas aeruginosa* mutants. *Gene*. 212:77-86.
- Holt, J.G. 1994. Bergy's Manual of Bacteriology. Lippincott Williams & Wilkins, Philadelphia, PA.
- Holtje, J.V. 1995. From growth to autolysis: the murein hydrolases in *Escherichia coli*. *Archives of Microbiology*. 164:243-254.
- Holtje, J.V., D. Mirelman, N. Sharon, and U. Schwarz. 1975. Novel type of murein transglycosylase in *Escherichia coli*. *Journal of Bacteriology*. 124:1067-1076.

- Huang, K.C., and K.S. Ramamurthi. 2010. Macromolecules that prefer their membranes curvy. *Molecular Microbiology*. 76:822-832.
- Iwai, N., K. Nagai, and M. Wachi. 2002. Novel S-benzylisothiourea compound that induces spherical cells in *Escherichia coli* probably by acting on a rod-shape-determining protein(s) other than penicillin-binding protein 2. *Bioscience, Biotechnology, and Biochemistry*. 66:2658-2662.
- Juan, C., B. Moya, J.L. Perez, and A. Oliver. 2006. Stepwise upregulation of the *Pseudomonas aeruginosa* chromosomal cephalosporinase conferring high-level beta-lactam resistance involves three AmpD homologues. *Antimicrobial Agents and Chemotherapy*. 50:1780-1787.
- Kelley, L.A., and M.J. Sternberg. 2009. Protein structure prediction on the Web: a case study using the Phyre server. *Nature Protocols*. 4:363-371.
- Kerff, F., S. Petrella, F. Mercier, E. Sauvage, R. Herman, A. Pennartz, A. Zervosen, A. Luxen, J.M. Frere, B. Joris, and P. Charlier. 2010. Specific structural features of the N-acetylmuramoyl-L-alanine amidase AmiD from *Escherichia coli* and mechanistic implications for enzymes of this family. *Journal of Molecular Biology*. 397:249-259.

- Koch, A.L., and S. Woeste. 1992. Elasticity of the sacculus of *Escherichia coli*. *Journal of Bacteriology*. 174:4811-4819.
- Kohanski, M.A., D.J. Dwyer, and J.J. Collins. 2010. How antibiotics kill bacteria: from targets to networks. *Nature Reviews. Microbiology*. 8:423-435.
- Korza, H.J., and M. Bochtler. 2005. Pseudomonas aeruginosa LD-carboxypeptidase, a serine peptidase with a Ser-His-Glu triad and a nucleophilic elbow. *The Journal of Biological Chemistry*. 280:40802-40812.
- Labedan, B., and M. Riley. 1995. Widespread protein sequence similarities: origins of *Escherichia coli* genes. *Journal of Bacteriology*. 177:1585-1588.
- Lambert, P.A. 2002. Mechanisms of antibiotic resistance in *Pseudomonas aeruginosa*. *Journal of the Royal Society of Medicine*. 95 Suppl 41:22-26.
- Lange, R., and R. Hengge-Aronis. 1994. The nlpD gene is located in an operon with *rpoS* on the *Escherichia coli* chromosome and encodes a novel lipoprotein with a potential function in cell wall formation. *Molecular Microbiology*. 13:733-743.

Lee, M., W. Zhang, D. Heseck, B.C. Noll, B. Boggess, and S. Mobashery. 2009. Bacterial AmpD at the crossroads of peptidoglycan recycling and manifestation of antibiotic resistance. *Journal of the American Chemical Society*. 131:8742-8743.

Lee, Y.J., H.Y. Liu, Y.C. Lin, K.L. Sun, C.L. Chun, and P.R. Hsueh. 2010. Fluoroquinolone resistance of *Pseudomonas aeruginosa* isolates causing nosocomial infection is correlated with levofloxacin but not ciprofloxacin use. *International Journal of Antimicrobial Agents*. 35:261-264.

Li, Y., J. Hsin, L. Zhao, Y. Cheng, W. Shang, K.C. Huang, H.W. Wang, and S. Ye. 2013. FtsZ protofilaments use a hinge-opening mechanism for constrictive force generation. *Science*. 341:392-395.

Lister, P.D., D.J. Wolter, and N.D. Hanson. 2009. Antibacterial-resistant *Pseudomonas aeruginosa*: clinical impact and complex regulation of chromosomally encoded resistance mechanisms. *Clinical Microbiology Reviews*. 22:582-610.

Loose, M., K. Kruse, and P. Schwille. 2011. Protein self-organization: lessons from the min system. *Annual Review of Biophysics*. 40:315-336.

Lowe, J., and L.A. Amos. 1998. Crystal structure of the bacterial cell-division protein FtsZ. *Nature*. 391:203-206.

- Lupoli, T.J., T. Taniguchi, T.S. Wang, D.L. Perlstein, S. Walker, and D.E. Kahne. 2009. Studying a cell division amidase using defined peptidoglycan substrates. *Journal of the American Chemical Society*. 131:18230-18231.
- Lutkenhaus, J. 2009. FtsN--trigger for septation. *Journal of Bacteriology*. 191:7381-7382.
- Mainardi, J.L., M. Fourgeaud, J.E. Hugonnet, L. Dubost, J.P. Brouard, J. Ouazzani, L.B. Rice, L. Gutmann, and M. Arthur. 2005. A novel peptidoglycan cross-linking enzyme for a beta-lactam-resistant transpeptidation pathway. *The Journal of Biological Chemistry*. 280:38146-38152.
- Markiewicz, Z., B. Glauner, and U. Schwarz. 1983. Murein structure and lack of DD- and LD-carboxypeptidase activities in *Caulobacter crescentus*. *Journal of Bacteriology*. 156:649-655.
- Matias, V.R., A. Al-Amoudi, J. Dubochet, and T.J. Beveridge. 2003. Cryo-transmission electron microscopy of frozen-hydrated sections of *Escherichia coli* and *Pseudomonas aeruginosa*. *Journal of Bacteriology*. 185:6112-6118.
- Meinhardt, H., and P.A. de Boer. 2001. Pattern formation in *Escherichia coli*: a model for the pole-to-pole oscillations of Min proteins and the localization of the division

site. *Proceedings of the National Academy of Sciences of the United States of America*. 98:14202-14207.

Mellroth, P., and H. Steiner. 2006. PGRP-SB1: an N-acetylmuramoyl L-alanine amidase with antibacterial activity. *Biochemical and Biophysical Research Communications*. 350:994-999.

Mohammadi, T., A. Karczmarek, M. Crouvoisier, A. Bouhss, D. Mengin-Lecreulx, and T. den Blaauwen. 2007. The essential peptidoglycan glycosyltransferase MurG forms a complex with proteins involved in lateral envelope growth as well as with proteins involved in cell division in *Escherichia coli*. *Molecular Microbiology*. 65:1106-1121.

Mohammadi, T., V. van Dam, R. Sijbrandi, T. Vernet, A. Zapun, A. Bouhss, M. Diepeveen-de Bruin, M. Nguyen-Disteche, B. de Kruijff, and E. Breukink. 2011. Identification of FtsW as a transporter of lipid-linked cell wall precursors across the membrane. *The EMBO Journal*. 30:1425-1432.

Moya, B., C. Juan, S. Alberti, J.L. Perez, and A. Oliver. 2008. Benefit of having multiple ampD genes for acquiring beta-lactam resistance without losing fitness and virulence in *Pseudomonas aeruginosa*. *Antimicrobial Agents and Chemotherapy*. 52:3694-3700.

- Peters, N.T., T. Dinh, and T.G. Bernhardt. 2011. A fail-safe mechanism in the septal ring assembly pathway generated by the sequential recruitment of cell separation amidases and their activators. *Journal of Bacteriology*. 193:4973-4983.
- Peters, N.T., C. Morlot, D.C. Yang, T. Uehara, T. Vernet, and T.G. Bernhardt. 2013. Structure-function analysis of the LytM domain of EnvC, an activator of cell wall remodelling at the *Escherichia coli* division site. *Molecular Microbiology*.
- Pichoff, S., and J. Lutkenhaus. 2002. Unique and overlapping roles for ZipA and FtsA in septal ring assembly in *Escherichia coli*. *The EMBO Journal*. 21:685-693.
- Pichoff, S., and J. Lutkenhaus. 2005. Tethering the Z ring to the membrane through a conserved membrane targeting sequence in FtsA. *Molecular Microbiology*. 55:1722-1734.
- Poggio, S., C.N. Takacs, W. Vollmer, and C. Jacobs-Wagner. 2010. A protein critical for cell constriction in the Gram-negative bacterium *Caulobacter crescentus* localizes at the division site through its peptidoglycan-binding LysM domains. *Molecular Microbiology*. 77:74-89.

- Priyadarshini, R., D.L. Popham, and K.D. Young. 2006. Daughter cell separation by penicillin-binding proteins and peptidoglycan amidases in *Escherichia coli*. *Journal of Bacteriology*. 188:5345-5355.
- Projan, S.J. 2002. New (and not so new) antibacterial targets - from where and when will the novel drugs come? *Current Opinion in Pharmacology*. 2:513-522.
- Quintela, J.C., M. Caparros, and M.A. de Pedro. 1995. Variability of peptidoglycan structural parameters in gram-negative bacteria. *FEMS Microbiology Letters*. 125:95-100.
- Ramadurai, L., K.J. Lockwood, M.J. Nadakavukaren, and R.K. Jayaswal. 1999. Characterization of a chromosomally encoded glycylglycine endopeptidase of *Staphylococcus aureus*. *Microbiology*. 145 (Pt 4):801-808.
- Rico, A.I., M. Garcia-Ovalle, P. Palacios, M. Casanova, and M. Vicente. 2010. Role of *Escherichia coli* FtsN protein in the assembly and stability of the cell division ring. *Molecular Microbiology*. 76:760-771.
- Rigden, D.J., M.J. Jedrzejas, and M.Y. Galperin. 2003. Amidase domains from bacterial and phage autolysins define a family of gamma-D,L-glutamate-specific amidohydrolases. *Trends in Biochemical Sciences*. 28:230-234.

- Rost, B. 1999. Twilight zone of protein sequence alignments. *Protein Engineering*. 12:85-94.
- Rudner, D.Z., and R. Losick. 2010. Protein subcellular localization in bacteria. *Cold Spring Harbor perspectives in biology*. 2:000307.
- Sabala, I., I.M. Jonsson, A. Tarkowski, and M. Bochtler. 2012. Anti-staphylococcal activities of lysostaphin and LytM catalytic domain. *BMC Microbiology*. 12:97.
- Sauvage, E., F. Kerff, M. Terrak, J.A. Ayala, and P. Charlier. 2008. The penicillin-binding proteins: structure and role in peptidoglycan biosynthesis. *FEMS Microbiology Reviews*. 32:234-258.
- Scheurwater, E.M., J.M. Pfeffer, and A.J. Clarke. 2007. Production and purification of the bacterial autolysin N-acetylmuramoyl-L-alanine amidase B from *Pseudomonas aeruginosa*. *Protein Expression and Purification*. 56:128-137.
- Shida, T., H. Hattori, F. Ise, and J. Sekiguchi. 2001. Mutational analysis of catalytic sites of the cell wall lytic N-acetylmuramoyl-L-alanine amidases CwlC and CwlV. *The Journal of Biological Chemistry*. 276:28140-28146.

- Shih, Y.L., and M. Zheng. 2013. Spatial control of the cell division site by the Min system in *Escherichia coli*. *Environmental Microbiology*.
- Smith, T.J., S.A. Blackman, and S.J. Foster. 2000. Autolysins of *Bacillus subtilis*: multiple enzymes with multiple functions. *Microbiology*. 146 (Pt 2):249-262.
- Steen, A., G. Buist, K.J. Leenhouts, M. El Khattabi, F. Grijpstra, A.L. Zomer, G. Venema, O.P. Kuipers, and J. Kok. 2003. Cell wall attachment of a widely distributed peptidoglycan binding domain is hindered by cell wall constituents. *The Journal of Biological Chemistry*. 278:23874-23881.
- Uehara, T., and T.G. Bernhardt. 2011. More than just lysins: peptidoglycan hydrolases tailor the cell wall. *Current Opinion in Microbiology*. 14:698-703.
- Uehara, T., T. Dinh, and T.G. Bernhardt. 2009. LytM-domain factors are required for daughter cell separation and rapid ampicillin-induced lysis in *Escherichia coli*. *Journal of Bacteriology*. 191:5094-5107.
- Uehara, T., K.R. Parzych, T. Dinh, and T.G. Bernhardt. 2010. Daughter cell separation is controlled by cytokinetic ring-activated cell wall hydrolysis. *The EMBO Journal*. 29:1412-1422.

- van Berkel, S.S., J. Brem, A.M. Rydzik, R. Salimraj, R. Cain, A. Verma, R.J. Owens, C.W. Fishwick, J. Spencer, and C.J. Schofield. 2013. An assay platform for clinically relevant metallo-beta-lactamases. *Journal of Medicinal Chemistry*.
- van den Ent, F., T.M. Vinkenvleugel, A. Ind, P. West, D. Veprintsev, N. Nanninga, T. den Blaauwen, and J. Lowe. 2008. Structural and mutational analysis of the cell division protein FtsQ. *Molecular Microbiology*. 68:110-123.
- van Heijenoort, J. 2001. Formation of the glycan chains in the synthesis of bacterial peptidoglycan. *Glycobiology*. 11:25R-36R.
- Vazquez-Laslop, N., H. Lee, R. Hu, and A.A. Neyfakh. 2001. Molecular sieve mechanism of selective release of cytoplasmic proteins by osmotically shocked *Escherichia coli*. *Journal of Bacteriology*. 183:2399-2404.
- Veesenmeyer, J.L., A.R. Hauser, T. Lisboa, and J. Rello. 2009. *Pseudomonas aeruginosa* virulence and therapy: evolving translational strategies. *Critical Care Medicine*. 37:1777-1786.
- Vollmer, W., and U. Bertsche. 2008. Murein (peptidoglycan) structure, architecture and biosynthesis in *Escherichia coli*. *Biochimica et Biophysica Acta*. 1778:1714-1734.

- Vollmer, W., D. Blanot, and M.A. de Pedro. 2008. Peptidoglycan structure and architecture. *FEMS Microbiology Reviews*. 32:149-167.
- Vollmer, W., B. Joris, P. Charlier, and S. Foster. 2008. Bacterial peptidoglycan (murein) hydrolases. *FEMS Microbiology Reviews*. 32:259-286.
- Vollmer, W., and S.J. Seligman. 2010. Architecture of peptidoglycan: more data and more models. *Trends in Microbiology*. 18:59-66.
- Wientjes, F.B., C.L. Woldringh, and N. Nanninga. 1991. Amount of peptidoglycan in cell walls of Gram-negative bacteria. *Journal of Bacteriology*. 173:7684-7691.
- Wissel, M.C., and D.S. Weiss. 2004. Genetic analysis of the cell division protein FtsI (PBP3): amino acid substitutions that impair septal localization of FtsI and recruitment of FtsN. *Journal of Bacteriology*. 186:490-502.
- Yang, D.C., N.T. Peters, K.R. Parzych, T. Uehara, M. Markovski, and T.G. Bernhardt. 2011. An ATP-binding cassette transporter-like complex governs cell-wall hydrolysis at the bacterial cytokinetic ring. *Proceedings of the National Academy of Sciences of the United States of America*. 108:E1052-1060.

- Yang, D.C., K. Tan, A. Joachimiak, and T.G. Bernhardt. 2012. A conformational switch controls cell wall-remodelling enzymes required for bacterial cell division. *Molecular Microbiology*. 85:768-781.
- Yao, X., M. Jericho, D. Pink, and T. Beveridge. 1999. Thickness and elasticity of Gram-negative murein sacculi measured by atomic force microscopy. *Journal of Bacteriology*. 181:6865-6875.
- Young, K.D. 2003. Bacterial shape. *Molecular Microbiology*. 49:571-580.
- Yu, X.C., A.H. Tran, Q. Sun, and W. Margolin. 1998. Localization of cell division protein FtsK to the *Escherichia coli* septum and identification of a potential N-terminal targeting domain. *Journal of Bacteriology*. 180:1296-1304.